

Perturbation theory of optical resonances of deformed dielectric spheres

Andrea Aiello,^{1,2,*} Jack G. E. Harris,³ and Florian Marquardt^{1,2}

¹*Institute for Theoretical Physics, Department of Physics, University of Erlangen-Nürnberg, Staudtstrasse 7, 91058 Erlangen, Germany*

²*Max Planck Institute for the Science of Light, Staudtstrasse 2, 91058 Erlangen, Germany*

³*Department of Physics, Yale University, New Haven, Connecticut 06520, USA*



(Received 7 September 2018; revised manuscript received 30 July 2019; published 23 August 2019)

We analyze the optical resonances of a dielectric sphere the surface of which has been slightly deformed in an arbitrary way. Setting up a perturbation series up to second order, we derive both the frequency shifts and the modified linewidths. Our theory is applicable, for example, to freely levitated liquid drops or solid spheres, which are deformed by thermal surface vibrations, centrifugal forces, or arbitrary surface waves. A dielectric sphere is effectively an open system the description of which requires the introduction of non-Hermitian operators characterized by complex eigenvalues and non-normalizable eigenfunctions. We avoid these difficulties using the Kapur-Peierls formalism, which enables us to extend the popular Rayleigh-Schrödinger perturbation theory to the case of electromagnetic Debye potentials describing the light fields inside and outside the near-spherical dielectric object. We find analytical formulas, valid within certain limits, for the deformation-induced first- and second-order corrections to the central frequency and bandwidth of a resonance. As an application of our method, we compare our results with preexisting ones, finding full agreement.

DOI: [10.1103/PhysRevA.100.023837](https://doi.org/10.1103/PhysRevA.100.023837)

I. INTRODUCTION

In this paper we address the problem of determining the optical resonances of slightly deformed dielectric spheres. Inside an almost spherical dielectric body embedded in vacuum or air, light is confined by near-total internal reflection and propagates with little attenuation along the inner surface of the body. This form of propagation is denoted as whispering gallery modes, which are typically characterized by a high quality factor Q [1]. For a perfect (ideal) dielectric sphere in air or vacuum, with a radius of a few millimeters, the predicted Q can easily exceed 10^{20} at optical frequencies. However, several physical processes (among which scattering from surface roughness can be the most prominent) limit the effective value of Q to about $10^8 - 10^9$ [2,3]. Our goal is to develop a perturbation theory that allows us to calculate the Q factors of the optical resonances of dielectric spheres the surfaces of which are slightly deformed by various physical processes.

The study of light interacting with spherical or near-spherical dielectric bodies dates back to Aristotle, who first described (although incorrectly) the rainbow as due to light reflection from raindrops [4]. In much more recent times microscopic glass spheres have been widely used as passive and active optical resonators in linear and nonlinear optics regimes for numerous physical, chemical, and biological applications (see, e.g., [5,6] and references therein). Recently, dielectric optical resonators of many diverse shapes have been regarded as optomechanical systems [7,8]. Even more recently, optomechanical devices consisting of drops of var-

ious liquid materials have been proposed and demonstrated [9–11]. In these devices the near-spherical free surface of the drop provides for both the optical and the mechanical resonators. As an example thereof, we have suggested the use of millimeter-scale drops of superfluid He magnetically levitated in vacuum as a novel type of optomechanical device [11]. The surface of a levitated drop may differ from a perfect sphere for several reasons, as shown in Fig. 1. For example, a rotating liquid drop is squeezed along the axis of rotation and takes the form of an oblate spheroid. On top of this, thermally excited capillary waves (ripples) will result in corrugations upon the droplet's surface.

All these optical and optomechanical devices are describable as *open systems*, that is, physical systems that leak energy via the coupling with an external environment [12]. The mathematical description of either classical or quantum open systems requires the use of non-Hermitian operators, which are characterized by complex-valued eigenvalues [13–15]. One important challenge with non-Hermitian operators is that they may not possess a set of orthonormal eigenfunctions. This implies that the familiar Rayleigh-Schrödinger perturbation theory is no longer applicable and different methods must be used.

Among these methods, the quasi-stationary-states approach and the Kapur-Peierls (KP) formalism are quite popular [16]. Quasistationary (Gamow or Siegert functions [17,18]) states are solutions of a wave equation with purely outgoing boundary conditions and can be used to build a perturbation theory called “resonant-state expansion (RSE)” [19]. In optics, the RSE technique has been put forward in [20] and successfully applied to three-dimensional dielectric resonators in [21]. However, basically the same method was already used in [22] to find optical resonances in microdroplets

*andrea.aiello@mpl.mpg.de

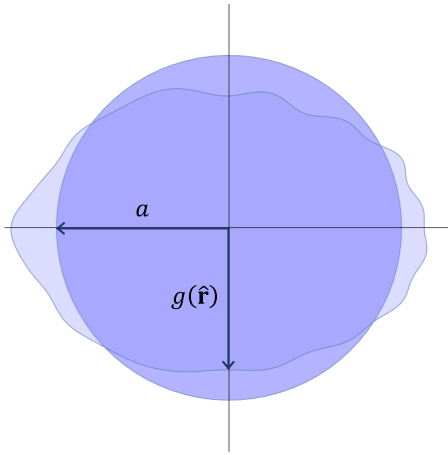


FIG. 1. Cartoonlike representation of the cross-section of a dielectric sphere with its deformations. The nondeformed sphere is represented by a dark-blue disk of radius a . The irregular curve represents a generic quasospherical corrugated surface and it is characterized by the surface profile function $g(\hat{\mathbf{r}})$ (see Sec. IV A for details).

within first-order perturbation theory. The main problem with quasistationary states is that they are not orthonormal in the conventional sense and the standard normalization integral diverges [23,24].

Conversely, Kapur-Peierls theory is not affected by these normalization problems [25,26] and automatically furnishes a biorthogonal complete set of functions suitable for use in perturbation theory. This formalism was originally developed in the context of nuclear scattering theory and was recently applied to the study of the resonances of one- and two-dimensional open optical systems [27,28].

In this paper we use Kapur-Peierls formalism to develop a perturbation theory of optical resonances of three-dimensional open optical systems (near-spherical dielectric bodies), correct up to and including second-order terms. We find analytic formulas for the characteristic values (complex wave numbers) of these resonances and we apply our theory to dielectric spheres with various deformations.

The application we have in mind is a situation in which the wavelength is much smaller than the sphere's radius (e.g., 100 or 1000 times). In this case, which is of great experimental significance, the use of numerical techniques [like the ones routinely used in commercially available finite element method (FEM) solvers] becomes very challenging if not prohibitive. For this reason, we do not present comparison to FEM results in the present paper. However, we compare our results with the analytical predictions (limited to first-order perturbation theory) of previous works and find complete agreement.

The paper is organized as follows. In Sec. II we briefly describe what we regard as “the unperturbed problem,” namely, the determination of the optical resonances of a dielectric sphere using the formalism of Debye potentials and scattering theory. Then, in Sec. III we furnish a review of the Kapur-Peierls formalism, which sets the basis for the remainder. In Sec. IV we apply this formalism to develop a perturbation theory for the Debye potentials. In Sec. V we use Rayleigh-

Schrödinger perturbation theory to achieve the main goal of this paper, namely, finding the optical resonances of slightly deformed dielectric spheres. In Sec. VI we show three different applications of our theory. Finally, in Sec. VII we draw some conclusions.

II. RESONANCES OF A DIELECTRIC SPHERE

The mathematical problem of the interaction of electromagnetic waves with dielectric spheres is more than one century old and represents a vast literature. The standard reference is still Stratton's classic book [29]. However, a more modern and thorough exposition can be found in [30]. In this section we briefly review the so-called Debye potentials approach and establish the basic notation that we shall use throughout this paper.

A. Setting the problem

Consider a sphere of radius a made of a homogeneous isotropic dielectric medium (medium 1) surrounded by air or vacuum (medium 2). We use SI units with electric permittivity ϵ_0 , magnetic permeability μ_0 , and speed of light $c = 1/(\epsilon_0\mu_0)^{1/2}$ in vacuum. Let $\mathbf{E}_1, \mathbf{B}_1, \mathbf{D}_1, \mathbf{H}_1$ and $\mathbf{E}_2, \mathbf{B}_2, \mathbf{D}_2, \mathbf{H}_2$ denote the electromagnetic fields in medium 1 and medium 2, respectively. For our purposes it is sufficient to presume that all fields vary as $\exp(-i\omega t)$, where $\omega = kc$, k being the wave number of light in vacuum. These fields obey the Maxwell equations

$$\nabla \cdot \mathbf{D}_j = 0, \quad (1a)$$

$$\nabla \cdot \mathbf{B}_j = 0, \quad (1b)$$

$$i\omega \mathbf{D}_j + \nabla \times \mathbf{H}_j = 0, \quad (1c)$$

$$-i\omega \mathbf{B}_j + \nabla \times \mathbf{E}_j = 0 \quad (1d)$$

(here and hereafter $j = 1, 2$, unless stated otherwise) and the constitutive equations

$$\mathbf{D}_j = \epsilon_j \epsilon_0 \mathbf{E}_j, \quad \mathbf{B}_j = \mu_j \mu_0 \mathbf{H}_j, \quad (2)$$

with $\mu_1 = \mu_2 = 1$ (we assume that both media are nonmagnetic) and $\epsilon_1 = n_1^2$, $\epsilon_2 = n_2^2$, where $n_1 > 1$ is the real-valued refractive index of medium 1 and $n_2 = 1$ is the refractive index of air or vacuum. The assumption that the dielectric is nonmagnetic implies that there is no physical difference between the magnetic strength \mathbf{H} and the magnetic induction \mathbf{B} , so in the remainder we shall consider \mathbf{B} as the independent field.

Following [31], we express the solutions of the set of equations (1) in terms of the transverse electric (TE) and transverse magnetic (TM) Debye *scalar potentials* $\Psi_j(\mathbf{r})$ and $\Phi_j(\mathbf{r})$, respectively, as follows:

$$\mathbf{E}_j^{\text{TE}} = ik \nabla \times (\mathbf{r} \Psi_j), \quad (3)$$

$$c \mathbf{B}_j^{\text{TE}} = \nabla \times [\nabla \times (\mathbf{r} \Psi_j)]$$

and

$$\mathbf{E}_j^{\text{TM}} = \frac{i}{n_j^2} \nabla \times [\nabla \times (\mathbf{r} \Phi_j)], \quad (4)$$

$$c \mathbf{B}_j^{\text{TM}} = k \nabla \times (\mathbf{r} \Phi_j).$$

Equations (1) and (2) are automatically satisfied by the fields (3) and (4) when the Debye potentials obey the scalar Helmholtz equation

$$\nabla^2 U + k^2 n_j^2 U = 0, \quad (5)$$

where U denotes either Ψ_j or Φ_j . This equation must be completed by the interface conditions which require the continuity of tangential components of \mathbf{E} and \mathbf{H} (or \mathbf{B}) across the surface of the sphere [32], that is,

$$\begin{aligned} \hat{\mathbf{r}} \times (\mathbf{E}_2 - \mathbf{E}_1)|_{r=a} &= 0, \\ \hat{\mathbf{r}} \times (\mathbf{B}_2 - \mathbf{B}_1)|_{r=a} &= 0, \end{aligned} \quad (6)$$

where $r = |\mathbf{r}|$ and $\hat{\mathbf{r}} = \mathbf{r}/r$.

Because of the symmetry of the problem imposed by (6), it is convenient to solve the Helmholtz equation (5) in spherical coordinates (r, θ, ϕ) . Following [31] we rewrite the Laplace operator ∇^2 as

$$\nabla^2 U = \frac{1}{r} \frac{\partial^2}{\partial r^2} (rU) - \frac{\hat{L}^2}{r^2} U, \quad (7)$$

where $\hat{L}^2 \equiv \hat{\mathbf{L}} \cdot \hat{\mathbf{L}}$ with $\hat{\mathbf{L}} \equiv -i\mathbf{r} \times \nabla$. Now, we look for solutions of (5) of the form

$$\begin{aligned} \Psi_j(r, \theta, \phi) &= \frac{u_j(r)}{r} Y_{lm}(\theta, \phi), \\ \Phi_j(r, \theta, \phi) &= \frac{v_j(r)}{r} Y_{lm}(\theta, \phi), \end{aligned} \quad (8)$$

where $Y_{lm}(\theta, \phi)$ are the standard spherical harmonics [32] satisfying $\hat{L}^2 Y_{lm} = l(l+1)Y_{lm}$, and $u_j(r)$ and $v_j(r)$ denote the reduced radial Debye potentials. Substituting (8) into (5) and using (7), we obtain the ordinary differential equation

$$-\psi_j''(r) + \left[\frac{l(l+1)}{r^2} - k^2 n_j^2 \right] \psi_j(r) = 0, \quad (9)$$

where $\psi_j = u_j$ for TE polarization, $\psi_j = v_j$ for TM polarization, and $\psi_j'' \equiv d^2 \psi_j / dr^2$. This equation must be supplied with the interface conditions for the reduced radial potentials $\psi_j(r)$. Substituting (3) and (4) into (6) and using (8) we obtain

$$\psi_1(a) = \psi_2(a), \quad \psi_1'(a) = p \psi_2'(a), \quad (10)$$

where $\psi_j' \equiv d\psi_j/dr$ and here and hereafter $p = 1$ for TE polarization and $p = n_1^2/n_2^2$ for TM polarization. We remark that in the literature Eq. (9) is often written in a ‘‘quantumlike’’ form as

$$-\psi_j''(r) + \left[\frac{l(l+1)}{r^2} + V_j \right] \psi_j(r) = E \psi_j(r), \quad (11)$$

where $V_j = k^2(1 - n_j^2)$ and $E = k^2$ (see, e.g., [31,33]). We shall exploit this quantum-classical analogy in the next section.

B. Scattering solutions

The general solution of (9) can be written as

$$\psi_j(r) = C_1 r j_l(n_j k r) + C_2 r y_l(n_j k r), \quad (12)$$

where $j_l(z)$ and $y_l(z)$ are spherical Bessel functions of the first and second kind, respectively [34]. Using the spherical Hankel functions $h_l^{(1)}(z) = j_l(z) + i y_l(z)$ and $h_l^{(2)}(z) =$

$j_l(z) - i y_l(z)$, we can rewrite (12) as

$$\psi_j(r) = C_3 r h_l^{(1)}(n_j k r) + C_4 r h_l^{(2)}(n_j k r), \quad (13)$$

where $C_3 = (C_1 - iC_2)/2$ and $C_4 = (C_1 + iC_2)/2$. Since $j_l(z) \sim z^l$ and $n_l(z) \sim 1/z^{l+1}$ for $z \rightarrow 0$, while $h_l^{(1)}(z) \sim (-i)^{l+1} e^{iz}/z$ and $h_l^{(2)}(z) \sim i^{l+1} e^{-iz}/z$ for $z \rightarrow \infty$, the *everywhere regular* solutions to (9) are

$$\begin{aligned} \psi_1(r) &= A_l r j_l(n_1 k r), & r \leq a, \\ \psi_2(r) &= I r h_l^{(2)}(kr) + S_l r h_l^{(1)}(kr), & r > a, \end{aligned} \quad (14)$$

where I is the amplitude of the incident wave and S_l is that of the scattered wave with azimuthal index l . A_l is the amplitude of the same wave inside the sphere. Assuming only *outgoing waves* means setting $I = 0$. This choice leads to the so-called resonant-state formulation of scattering theory [20,21]. These states, also known in the quantum theory of scattering [16] as decaying, metastable, Gamow [17], or Siegert [18] states, are nonphysical because they are not normalizable in the standard manner (that is, they are not square integrable). Here we choose instead $I = 1$, which means assuming an *incident wave* of unit amplitude.

Substituting (14) into (10) we determine the interior wave amplitude

$$A_l(k) = \frac{2ip}{ka} \frac{1}{f_l(ka)} \quad (15)$$

and the scattering amplitude

$$S_l(k) = -\frac{f_l(-ka)}{f_l(ka)}, \quad (16)$$

where we have defined the Jost function [35]:

$$f_l(z) = p j_l(n_1 z) [z h_l^{(1)}(z)]' - h_l^{(1)}(z) [(n_1 z) j_l(n_1 z)]', \quad (17)$$

with the prime symbol ($'$) denoting the derivative with respect to the argument of the function, e.g., $[f(x)g(x)]' = (df/dx)g(x) + f(x)(dg/dx)$. Using (A4) it is straightforward to show that for k real $f_l(-ka) = f_l^*(ka)$ and we can write

$$S_l(k) = \exp[2i\delta_l(k)], \quad (18)$$

where $\delta_l(k)$ denotes the phase shift of the scattered wave [30]. In the absence of the dielectric sphere $n_1 = n_2 = 1$ and evidently scattering does not occur. In this case the equations above give $\delta_l = 0$, $S_l = 1$, and $A_l = 2$.

C. Resonances and Q factors

In Eqs. (15) and (16) k is the *real-valued* wave number of the ingoing wave. However, the resonances of the sphere are associated with the poles of the analytical continuation of $S_l(k)$ into the entire complex plane: $k \in \mathbb{R} \rightarrow k = k' + ik'' \in \mathbb{C}$, where here and hereafter $k' = \text{Re } k$ and $k'' = \text{Im } k$. The continuation of $S_l(k)$ is meromorphic, that is, analytic except at its poles. The latter are characterized by $\text{Im } k < 0$ and coincide with the roots of the transcendental equation

$$f_l(ka) = 0. \quad (19)$$

This equation, where l is a *fixed* number, has a denumerably infinite set of solutions denoted $\{k_{1l}, k_{2l}, \dots, k_{nl}, \dots\}$ the determination of which is detailed in Appendix B. From (A4)

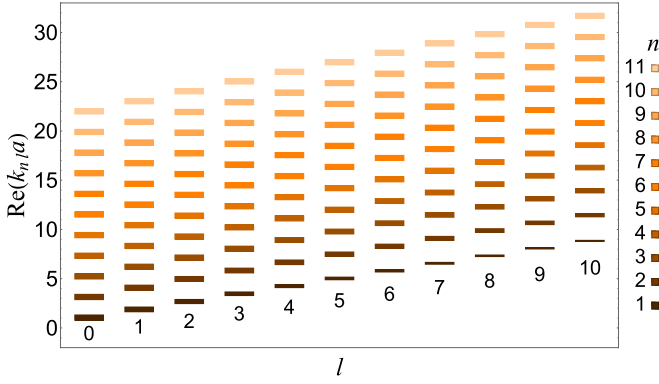


FIG. 2. Spectrum of the TE modes of a dielectric sphere of radius a and refractive index $n_1 = 1.5$. The values of k_{nl} for $1 \leq n \leq 11$ and $0 \leq l \leq 10$ are shown as orange bands. The vertical position of the center of each band is equal to $\text{Re}(k_{nl}a)$ and the thickness is equal to $\text{Im}(k_{nl}a)$. For the first radial mode $n = 1$ (darkest orange bands) the imaginary part of k_{nl} quickly decreases as l increases from left to right, while it decreases slowly for $n > 1$ radial modes. Each mode characterized by the pair of radial and azimuthal numbers (n, l) is $2l + 1$ times degenerate (see Sec. IV).

it follows that $f_l^*(z) = f_l(-z^*)$, that is, the resonance poles are located in the complex k plane in pairs symmetric with respect to the imaginary axis. Therefore, if k_{nl} is a solution of (19), then $-k_{nl}^*$ is also a solution. We label the poles with $\text{Re } k < 0$ by the negative index $-n$, so that $k_{-nl} = -k_{nl}^*$. A “central” pole labeled with $n = 0$ and characterized by $\text{Re } k_{0l} = 0$, $\text{Im } k_{0l} < 0$, exists only for l odd (even) and TE (TM) polarization. A portion of the spectrum of TE resonances of a dielectric sphere with refractive index $n_1 = 1.5$ is shown in Fig. 2.

Each resonance $k = k_{1l}, k_{2l}, \dots$, can be characterized by the quality factor Q defined by

$$Q(k', k'') \equiv -\frac{1}{2} \frac{\text{Re } k}{\text{Im } k} = -\frac{1}{2} \frac{k'}{k''}. \quad (20)$$

From this equation it follows that

$$\frac{\partial Q}{\partial k''} = 2Q \frac{\partial Q}{\partial k'}. \quad (21)$$

This means that Q is more sensitive to variations of losses ($\propto k''$) than of frequency ($\propto k'$), by a factor $2Q$. This is why also a tiny perturbation of k'' may cause a relevant variation of Q . This feature is relevant for the estimation of the variation of Q due to a small perturbation of the shape of the dielectric sphere.

The quality factor depends dramatically upon the value of l . For example, solving Eq. (19) numerically for a ^4He sphere with refractive index $n_1 \approx 1.03$ (superfluid He), $p = 1$ (TE polarization), $l = 4000$, and $l = 1000$, we have found $k_{1,4000}a \approx 4000/n_1 - i(2 \times 10^{-10})$ and $k_{1,1000}a \approx 1000/n_1 - i(1 \times 10^{-1})$, respectively, where we have chosen in both cases the first resonance labeled by $n = 1$. These values yield

$$Q(4000) = -\frac{1}{2} \frac{\text{Re}(k_{1,4000}a)}{\text{Im}(k_{1,4000}a)} \approx 10^{13}, \quad (22)$$

for $l = 4000$, and

$$Q(1000) = -\frac{1}{2} \frac{\text{Re}(k_{1,1000}a)}{\text{Im}(k_{1,1000}a)} \approx 5 \times 10^3, \quad (23)$$

for $l = 1000$. Thus, although l changes only by a factor of 4, the corresponding Q changes by about nine orders of magnitude. This huge variation in Q is largely determined by the imaginary parts of the resonances, because

$$\begin{aligned} \frac{Q(4000)}{Q(1000)} &= \frac{\text{Re}(k_{1,4000}a)}{\text{Re}(k_{1,1000}a)} \times \frac{\text{Im}(k_{1,1000}a)}{\text{Im}(k_{1,4000}a)} \\ &\approx \frac{4000}{1000} \times (2 \times 10^9). \end{aligned} \quad (24)$$

III. KAPUR-PEIERLS FORMALISM

In the previous section we have presented the standard theory of scattering from a piecewise constant spherically symmetric potential (dielectric sphere) and we have written Eq. (19) determining the resonances of the system [34]. This approach, based on the continuous (with respect to k) set of functions (14), is not very convenient for perturbation theory where it is desirable to deal with a denumerable set (a basis) of normalizable functions. The KP formalism, originally developed in the context of nuclear physics [25] and recently adapted to optical resonator theory [28,36], naturally yields a complete set of biorthogonal functions [37].

A. Preliminaries on the Kapur-Peierls formalism

Before starting our discussion, it is useful to briefly outline the general approach of KP perturbation theory. In the standard quantum-mechanics Rayleigh-Schrödinger time-independent perturbation theory, one first finds the full set of eigenstates of the Hamiltonian of the unperturbed system. Afterwards, the perturbative corrections to any one eigenstate can be expressed generically as sums over these eigenstates. In KP perturbation theory, the setting is slightly changed: One first solves an *auxiliary* eigenproblem the eigenvalues $\lambda(k)$ of which are functions of a continuous parameter, the complex scattering frequency (here represented by the complex wave number k). One then determines the discrete set of resonances in k by imposing $\lambda(k) = k^2$. Finally, the perturbative correction for a given resonance is obtained by summing over the previously obtained set of eigenstates that belongs to the resonance’s particular value of k . This makes the whole procedure more involved than Rayleigh-Schrödinger theory, since for each resonance we are dealing with a different set of infinitely many eigenstates (which are still loosely related to the whole set of resonances, but not identical to those).

Kapur-Peierls dispersion theory is well known within nuclear physics [38]. However, this formalism is much less known in the optics community. A useful purpose may therefore be served by shortly reviewing the Kapur-Peierls approach to scattering theory [39]. As in the previous section, we consider again the scattering of a scalar wave (any of the two Debye potentials) by a dielectric sphere; this simple example illustrates the main features of the theory and provides for the Kapur-Peierls eigenvalues and eigenfunctions characterizing the “unperturbed problem.” When the scatterer

is not perfectly spherical the simple theory presented in this section is no longer applicable and the use of perturbation theory becomes necessary. This will be presented in the next section.

We begin by rewriting (9) as

$$(\hat{D}_j - k^2)\psi_j(r) = 0, \quad (j = 1, 2), \quad (25)$$

where we have defined the differential operator

$$\hat{D}_j \equiv \frac{1}{n_j^2} \left[-\frac{d^2}{dr^2} + \frac{l(l+1)}{r^2} \right], \quad (26)$$

associated with the boundary conditions (10), that we rewrite as

$$\frac{\psi_1'(a)}{\psi_1(a)} = p \frac{\psi_2'(a)}{\psi_2(a)}, \quad (27)$$

where $p = 1$ for TE polarization and $p = n_1^2/n_2^2$ for TM polarization. We know from the previous section that the solution of (25) can be written for $r > a$ as

$$\psi_2(r) = I r h_l^{(2)}(kr) + S_l r h_l^{(1)}(kr), \quad (28)$$

which implies

$$\psi_2'(r) = I [(kr) h_l^{(2)}(kr)]' + S_l [(kr) h_l^{(1)}(kr)]', \quad (29)$$

where the prime symbol ($'$) denotes the derivative with respect to the argument of the function.

Kapur-Peierls theory is based upon the observation that using (28) and (29) we can express S_l and I via $\psi_2(a)$ and $\psi_2'(a)$ to obtain

$$\frac{S_l}{I} = -\frac{h_l^{(2)}(ka) \psi_2'(a) + c_l(-ka) \psi_2(a)}{h_l^{(1)}(ka) \psi_2'(a) - c_l(ka) \psi_2(a)}, \quad (30)$$

where

$$c_l(ka) \equiv \frac{1}{a} \frac{[(ka) h_l^{(1)}(ka)]'}{h_l^{(1)}(ka)}. \quad (31)$$

In Secs. II B and II C we have shown that the poles of the analytic continuation of $S_l(k)$, with $k = k' + ik''$, determine the resonances of the systems. From (30) it follows that these poles occur when the denominator vanishes, that is, when $\psi_2'(a) - c_l(ka)\psi_2(a) = 0$. Evidently, this happens when there is no incident wave, that is, $I = 0$, and the ratio S_l/I becomes singular. Using the boundary conditions (27) we can transform the relation $\psi_2'(a) - c_l(ka)\psi_2(a) = 0$ into the equivalent one:

$$\psi_1'(a) - p c_l(ka) \psi_1(a) = 0. \quad (32)$$

This implies that we can determine the resonances of the system by knowing the solutions $\psi_1(r)$ of the interior problem $(\hat{D}_1 - k^2)\psi_1(r) = 0$ with boundary conditions (32). We shall give a constructive proof of this statement in Sec. III C by deriving the so-called dispersion formula for the scattering amplitude $S_l(k)$. However, first we need to prove some basic results.

B. The Kapur-Peierls eigenfunctions

Let us consider the auxiliary eigenvalue problem

$$(\hat{D}_1 - \lambda_{nl}(k))\phi_{nl}(k, r) = 0, \quad r \leq a, \quad (33)$$

with boundary conditions

$$\phi_{nl}(k, 0) = 0, \quad \phi_{nl}'(k, a) - p c_l(ka) \phi_{nl}(k, a) = 0, \quad (34)$$

where n is a discrete numerical index, $\phi_{nl}(k, r)$ are the so-called Kapur-Peierls (right) eigenfunctions with $\phi_{nl}'(k, a) \equiv [d\phi_{nl}(k, r)/dr]_{r=a}$, and $c_l(ka)$ is given by (31). The (right) eigenvalues $\lambda_{nl}(k)$ depend on the parameter k via the boundary conditions (34). Here and hereafter k must be regarded as a fixed constant, the same for all eigenvalues $\lambda_{1l}(k), \lambda_{2l}(k), \dots$, which are complex numbers on account of the boundary condition (34). The normalized solutions of (33) are

$$\phi_{nl}(k, r) = \frac{1}{\sqrt{Z_{nl}}} r j_l(n_1 q_{nl} r), \quad (35)$$

where $q_{nl} = \sqrt{\lambda_{nl}(k)}$ and

$$Z_{nl} = \frac{a^3}{2} [j_l^2(n_1 q_{nl} a) - j_{l-1}(n_1 q_{nl} a) j_{l+1}(n_1 q_{nl} a)]. \quad (36)$$

The eigenvalues are given by $\lambda_{nl}(k) = z_{nl}^2/(n_1 a)^2$, where $\{z_{1l}, z_{2l}, \dots, z_{nl}, \dots\}$ are the complex roots of the k -dependent transcendental equation $F_l(z, ka) = 0$, where

$$F_l(z, w) = p j_l(z) [w h_l^{(1)}(w)]' - h_l^{(1)}(w) [z j_l(z)]'. \quad (37)$$

From (A2) it follows that if z_{nl} is a solution of (37) then $-z_{nl}$ is also a solution and both z_{nl} and $-z_{nl}$ yield the same eigenvalue $\lambda_{nl}(k)$. Different values of k produce different eigenvalues; typically $\lambda_{nl}(k) \neq \lambda_{nl}(k')$ for $k \neq k'$.

The operator defined by (33) and (34) is *not* self-adjoint because $c_l(ka)$ is a complex number. This implies that there exist left eigenfunctions $\tilde{\phi}_{nl}(k, r)$ and left eigenvalues $\tilde{\lambda}_{nl}(k)$ defined by the so-called adjoint equation

$$(\hat{D}_1 - \tilde{\lambda}_{nl}(k))\tilde{\phi}_{nl}(k, r) = 0, \quad r \leq a \quad (38)$$

and the adjoint boundary conditions

$$\tilde{\phi}_{nl}(k, 0) = 0, \quad \tilde{\phi}_{nl}'(k, a) - p c_l^*(ka) \tilde{\phi}_{nl}(k, a) = 0. \quad (39)$$

It is not difficult to show that $\tilde{\lambda}_{nl}(k) = \lambda_{nl}(k) = [\lambda_{nl}(-k^*)]^*$ and $\tilde{\phi}_{nl}(k, r) = \phi_{nl}^*(k, r) = \phi_{nl}(-k^*, r)$ [37]. Moreover, our normalization (36) yields

$$\begin{aligned} \int_0^a \tilde{\phi}_{n'l}^*(k, r) \phi_{nl}(k, r) dr &= \int_0^a \phi_{n'l}(k, r) \phi_{nl}(k, r) dr \\ &= \delta_{nn'}. \end{aligned} \quad (40)$$

This equation shows that the normalized Kapur-Peierls eigenfunctions $\phi_{nl}(k, r)$ belong to a biorthogonal set of functions.

Typically the functions $\phi_{nl}(k, r)$ form a complete set [26,40], that is,

$$\begin{aligned} \sum_n \phi_{nl}(k, r) \tilde{\phi}_{n'l}^*(k, r') &= \sum_n \phi_{nl}(k, r) \phi_{nl}(k, r') \\ &= \delta(r - r'), \end{aligned} \quad (41)$$

but usually this is not easy to prove (see, e.g., [41] for a discussion). For our functions (35) we have not been able to evaluate the left side of this equation analytically, but numerical evaluation for some values of l and k confirmed the validity of (41). Therefore, we assume without demonstration the completeness of the Kapur-Peierls functions (35).

C. The Kapur-Peierls dispersion formula

From (27)–(29) it follows that the interior function $\psi_1(r)$ obeys the boundary conditions

$$\psi_1'(a) - p c_l(ka) \psi_1(a) = I \frac{2p}{i \xi_l(ka)}, \quad (42)$$

where we have introduced the Riccati-Bessel functions $\xi_l(x) \equiv x h_l^{(1)}(x)$ and $\zeta_l(x) \equiv x h_l^{(2)}(x)$ [42]. These conditions reduce to (32) when no incident wave is present and $I = 0$. Consider then the auxiliary functions $\varphi_1(r)$ and $\varphi_2(r)$ defined by

$$\varphi_j(r) \equiv \psi_j(r) - X(r), \quad (j = 1, 2), \quad (43)$$

where $X(r)$ is any function satisfying the constraint

$$X'(a) - p c_l(ka) X(a) = I \frac{2p}{i \xi_l(ka)}. \quad (44)$$

It is then evident that $\varphi_1(a)$ obeys the same boundary conditions (34) satisfied by the Kapur-Peierls functions, that is,

$$\varphi_1'(a) - p c_l(ka) \varphi_1(a) = 0. \quad (45)$$

Therefore, using (41) and (43) we can write

$$\varphi_1(r) = \sum_n a_n \phi_{nl}(k, r), \quad (46)$$

where

$$\begin{aligned} a_n &= \int_0^a \phi_{nl}(k, r) [\psi_1(r) - X(r)] dr \\ &\equiv b_n - c_n. \end{aligned} \quad (47)$$

From (25) and (26) and using $\psi_1(0) = 0 = \phi_{nl}(k, 0)$, we obtain

$$\begin{aligned} b_n &= \int_0^a \phi_{nl}(k, r) \psi_1(r) dr \\ &= \int_0^a \frac{[\hat{D}_1 \phi_{nl}(k, r)] \psi_1(r) - \phi_{nl}(k, r) [\hat{D}_1 \psi_1(r)]}{\lambda_{nl}(k) - k^2} dr \\ &= \frac{1}{n_1^2} \frac{\phi_{nl}(k, a)}{\lambda_{nl}(k) - k^2} [\psi_1'(a) - p c_l(ka) \psi_1(a)]. \end{aligned} \quad (48)$$

Subtracting $X(a)$ from both sides of the matching condition $\psi_2(a) = \psi_1(a)$ we obtain $\varphi_2(a) = \varphi_1(a)$. Using (28), (46), and (47) we can rewrite this equation as

$$\begin{aligned} &\frac{1}{k} [I \zeta_l(ka) + S_l \xi_l(ka)] - X(a) \\ &= \sum_n b_n \phi_{nl}(k, a) - \sum_n c_n \phi_{nl}(k, a). \end{aligned} \quad (49)$$

Substituting (48) into (49) and using (42) gives

$$\begin{aligned} \frac{1}{k} [I \zeta_l(ka) + S_l \xi_l(ka)] &= -I \frac{p}{n_1^2} \frac{2i}{\xi_l(ka)} \sum_n \frac{\phi_{nl}(k, a)}{\lambda_{nl}(k) - k^2} \\ &\quad + \left[X(a) - \sum_n c_n \phi_{nl}(k, a) \right]. \end{aligned} \quad (50)$$

Since $X(r)$ is arbitrary and the condition (44) involves both $X(a)$ and $X'(a)$, we can always choose $X(r)$ such that $X(a) = \sum_n c_n \phi_{nl}(k, a)$ to cancel the last term in (50), and $X'(a)$ in a

manner that (44) becomes an identity. Then, solving (50) for S_l , we obtain

$$\frac{S_l}{I} = -\frac{\zeta_l(ka)}{\xi_l(ka)} [1 + 2i k R_l(k)], \quad (51)$$

where

$$R_l(k) = \frac{p}{n_1^2} \frac{1}{\xi_l(ka) \zeta_l(ka)} \sum_n \frac{\phi_{nl}^2(k, a)}{\lambda_{nl}(k) - k^2}, \quad (52)$$

and $p = 1$ for TE polarization and $p = n_1^2/n_2^2$ for TM polarization. It should be noticed that the sum in (52) is simply equal to -1 times the Green's function $G_l(k, r', r)$ for the internal problem $r', r \leq a$, evaluated at $r' = r = a$ [37]. We shall use this property later in Sec. V.

Equations (51) and (52) are an example of what is usually called a “dispersion formula” in nuclear physics. They give an explicit expression of the scattering amplitude S_l in terms of its singularities (poles). In particular, (52) provides for a practical recipe to find resonances: first we calculate the Kapur-Peierls eigenvalues $\lambda_{nl}(k)$ by solving (often numerically) the transcendental equation $F_l(n_1 a \sqrt{\lambda_{nl}(k)}, ka) = 0$ to determine $\sqrt{\lambda_{nl}(k)}$. Then, we look for the roots of the fixed-point equation

$$\sqrt{\lambda_{nl}(k)} = k. \quad (53)$$

It is understood that the only physically acceptable branch of the multivalued function $\sqrt{\lambda_{nl}(k)}$ is the one with $\text{Im} \sqrt{\lambda_{nl}(k)} < 0$. It is evident that (53) reproduces the resonance equation (19). To show this we must simply substitute, consistently with (53), $n_1 a \sqrt{\lambda_{nl}(k)}$ with $n_1 a k$ in $F_l(n_1 a \sqrt{\lambda_{nl}(k)}, ka) = 0$. This makes (37) coincident with (19), that is, $F_l(z, z) = f_l(z)$.

We remark that for a fixed value of the index n there may be several different solutions $k_{1l}, k_{2l}, \dots, k_{sl}, \dots$, of (53) such that $\lambda_{nl}(k_{sl}) = k_{sl}^2$. An example thereof is reported in [37]. However, in our case we found via numerical evaluation of (53) that there is only one solution for fixed n ; this is illustrated in Fig. 3 for two particular cases. Therefore, in the remainder we choose the natural numeration of the resonances so that $s = n$ and $\lambda_{nl}(k_{nl}) = k_{nl}^2$.

IV. PERTURBATION THEORY FOR THE DEBYE POTENTIALS

In the previous section we have described the Kapur-Peierls formalism. This yields a biorthogonal and complete set of basis functions defined in the interior region of the dielectric sphere. The goal of this section is to develop a perturbation theory for the Helmholtz equation (5) using these functions.

A. Description of the deformations of the surface of a dielectric sphere

We assume that the sphere's free surface can be described in spherical coordinates $(r, \theta, \phi) \equiv (r, \hat{\mathbf{r}})$ by the equation $r - g(\hat{\mathbf{r}}) = 0$, where

$$g(\hat{\mathbf{r}}) \equiv a + ah(\hat{\mathbf{r}}) \quad (54)$$

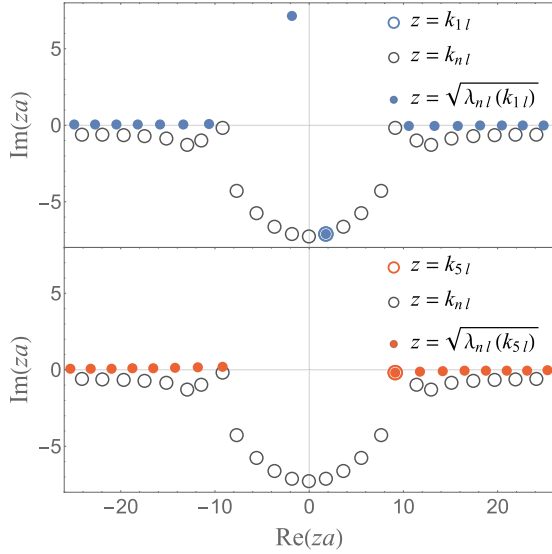


FIG. 3. Resonances k of an unperturbed sphere, and discrete eigenvalues of the Kapur-Peierls equation for two different values of k . The top plot displays the location of the roots $\{k_{nl}\}$ of (19) (open black circles) and (37) $\{\sqrt{\lambda_{nl}(k_{1l})}\}$ (filled blue circles) for $k = k_{1l}$. The root denoted k_{1l} (k_{0l} is the central root with $\text{Re } k_{0l} = 0$, k_{1l} is the right nearest root with $\text{Re } k_{1l} > 0$, k_{-1l} is the left nearest root with $\text{Re } k_{-1l} < 0$, etc.) is indicated by a blue open circle. It is evident that $\sqrt{\lambda_{nl}(k_{1l})} = k_{1l}$ for only one value of n . Similarly, the bottom plot displays the location of the roots of (19) (open black circles) and (37) $\{\sqrt{\lambda_{nl}(k_{5l})}\}$ (filled red circles) for $k = k_{5l}$. The root denoted k_{5l} is marked by a red open circle. Also here $\sqrt{\lambda_{nl}(k_{5l})} = k_{5l}$ for only one value of n . In both plots the field has TM polarization, $n_1 = 1.5$ and $l = 10$.

is the surface profile function and $a|h(\hat{\mathbf{r}})|$ describes the distance, in the direction $\hat{\mathbf{r}}$, of the *deformed* sphere surface from a *reference* unperturbed sphere of radius a . We suppose that for a given fixed direction $\hat{\mathbf{r}}$ the equation $r - g(\hat{\mathbf{r}}) = 0$ has only one solution. By definition, for a perfect sphere of radius a the profile function is constant, namely, $g(\hat{\mathbf{r}}) = a$ and $h(\hat{\mathbf{r}}) = 0$. Conversely, the surface profile function of the deformed sphere is effectively determined by

$$h(\hat{\mathbf{r}}) = \sum_{L=2}^{\infty} \sum_{M=-L}^L h_{LM} Y_{LM}(\hat{\mathbf{r}}), \quad (55)$$

where

$$h_{LM} = \int_0^{2\pi} d\phi \int_0^\pi d\theta \sin\theta Y_{LM}^*(\hat{\mathbf{r}}) h(\hat{\mathbf{r}}). \quad (56)$$

The relative permittivity $\epsilon_r(\mathbf{r})$ of the deformed sphere can be evidently described by the piecewise constant function

$$\epsilon_r(\mathbf{r}) = n_1^2 H[g(\hat{\mathbf{r}}) - r] + n_2^2 H[r - g(\hat{\mathbf{r}})], \quad (57)$$

where $H(x)$ denotes the Heaviside step function [43]. For a perfect sphere of radius a we define $\epsilon_r(\mathbf{r}) \equiv \epsilon_r^{(0)}(r) = n_1^2 H(a - r) + n_2^2 H(r - a)$. From $H(x) + H(-x) = 1$ it follows that we can rewrite $\epsilon_r(\mathbf{r})$ as the sum of the unperturbed permittivity $\epsilon_r^{(0)}(r)$ and a perturbation term $\Delta\epsilon_r(\mathbf{r})$:

$$\epsilon_r(\mathbf{r}) = \epsilon_r^{(0)}(r) + \Delta\epsilon_r(\mathbf{r}), \quad (58)$$

where

$$\Delta\epsilon_r(\mathbf{r}) = -(n_1^2 - n_2^2) \quad (59)$$

$$\{H[r - a + ah(\hat{\mathbf{r}})] - H(r - a)\}. \quad (60)$$

In the case of small deviations $|h(\hat{\mathbf{r}})| \ll 1$ from the reference spherical surface, we can approximate (59) with

$$\Delta\epsilon_r(\mathbf{r}) \cong (n_1^2 - n_2^2) \quad (61)$$

$$ah(\hat{\mathbf{r}}) \left[\delta(r - a) - \frac{ah(\hat{\mathbf{r}})}{2} \delta'(r - a) \right], \quad (62)$$

where $\delta'(r - a) = d\delta(r - a)/dr$ and we have expanded $\Delta\epsilon_r(\mathbf{r})$ to second order because we plan to calculate quadratic corrections to the resonant wave numbers. Evidently, there is a freedom in attributing the singular local terms in (61) to either the internal ($r \leq a$) or the external ($r > a$) region [36]. We choose to define $\Delta\epsilon_r(\mathbf{r})$ in the internal region solely. This implies that we can define an effective potential $V(\epsilon, \mathbf{r})$ as

$$V(\epsilon, \mathbf{r}) = \frac{\Delta\epsilon_r(\mathbf{r})}{n_1^2} \equiv \epsilon V^{(1)}(\mathbf{r}) + \epsilon^2 V^{(2)}(\mathbf{r}), \quad (63)$$

where $\epsilon \geq 0$ is a formal parameter serving to build a perturbation series with $V(0, \mathbf{r}) = 0$, and we have defined

$$V^{(1)}(\mathbf{r}) \equiv -v(k) ah(\hat{\mathbf{r}}) \delta(r - a), \quad (64)$$

$$V^{(2)}(\mathbf{r}) \equiv v(k) \frac{a^2 h^2(\hat{\mathbf{r}})}{2} \delta'(r - a),$$

with

$$v(k) \equiv k^2 (n_1^2 - n_2^2) / n_1^2. \quad (65)$$

A caveat is in order here. The Debye potentials representation presented in Sec. II A is valid for electromagnetic fields in *uniform* dielectric media. This condition is certainly satisfied by the physical dielectric bodies considered in this paper. However, the use of the potential (63) introduces an effective inhomogeneity at $r = a$. As the Debye potentials representation is still valid inside the dielectric body ($r < a$), in the spirit of perturbation theory it is reasonable to extend this representation to the whole region $r \leq a$, keeping in mind that this is an approximation.

B. Kapur-Peierls perturbation theory

According to the previous discussion, we consider now a perfect sphere the refractive index of which is modified by a small perturbation $V(\epsilon, \mathbf{r})$ defined for $r \leq a$ only. It must be put equal to 1 at the end of the calculations. Because of the both radial and angular dependence of V we have to generalize the radial equation (25) to

$$(\hat{D} - k^2)\Psi(\mathbf{r}) = 0, \quad (66)$$

where

$$\begin{aligned} \hat{D} &= \frac{1}{n_1^2} \left(-\frac{\partial^2}{\partial r^2} + \frac{\hat{L}^2}{r^2} \right) + V(\epsilon, \mathbf{r}) \\ &\equiv \hat{D}_0 + V(\epsilon, \mathbf{r}). \end{aligned} \quad (67)$$

As we deal with fields in the interior region only, in the remainder the index j will be omitted. The Kapur-Peierls eigenvalue equation for the unperturbed operator \hat{D}_0 reads as

$$[\hat{D}_0 - \lambda_{nl}(k)]\Phi_{nlm}(k, \mathbf{r}) = 0, \quad (68)$$

where

$$\Phi_{nlm}(k, \mathbf{r}) = \phi_{nl}(k, r)Y_{lm}(\theta, \phi), \quad (69)$$

and $\tilde{\Phi}_{nlm}(k, \mathbf{r}) = \tilde{\phi}_{nl}(k, r)Y_{lm}(\theta, \phi)$, with n , l , and m being the so-called radial, azimuthal, and magnetic numbers. The radial eigenfunctions $\phi_{nl}(k, r)$ are defined as before by (33)–(35). Since the boundary conditions (34) are independent of the magnetic number m , each eigenvalue $\lambda_{nl}(k)$ is $2l + 1$ times degenerate.

Now, suppose that $\epsilon \neq 0$. In this case when a wave with given radial, azimuthal, and magnetic numbers n , l , and m impinges upon the inhomogeneous dielectric sphere, it is scattered into many (possibly infinitely many) waves with different numbers n' , l' , and m' . This occurs because the nonspherically symmetric potential $V(\epsilon, \mathbf{r})$ couples different modes of the field [44]. Therefore, the “single-channel” Kapur-Peierls theory developed in the previous section is not directly applicable and the theory must be generalized (see, e.g., [25,38]). However, because of the spherically symmetric surface of the inhomogeneous dielectric body, we still have well-defined internal and external scattering regions characterized by $r \leq a$ and $r > a$, respectively. In this case it is not difficult to show [27] that the original Kapur-Peierls equation (33) can be replaced by the new eigenvalue equation

$$[\hat{D} - \Lambda_{nlm}(k)]\Psi_{nlm}(k, \mathbf{r}) = 0, \quad (70)$$

and the fixed-point equation (53) becomes

$$K_{nlm}^2 = \Lambda_{nlm}(K_{nlm}), \quad (71)$$

which must reduce to $k_{nl}^2 = \lambda_{nl}(k_{nl})$ for $\epsilon = 0$. However, it is important to keep in mind that while (53) is an *exact* relation Eq. (71) rests upon the approximation of replacing a near-spherical homogeneous dielectric body with an inhomogeneous spherical one.

Now, according to Rayleigh-Schrödinger perturbation theory suitably adapted to the case of a biorthogonal basis [13,15], we assume that $\Psi_{nlm}(k, \mathbf{r})$ and $\Lambda_{nlm}(k)$ can be expanded in powers of ϵ :

$$\Psi_{nlm}(k, \mathbf{r}) = \Psi_{nlm}^{(0)}(k, \mathbf{r}) + \epsilon \Psi_{nlm}^{(1)}(k, \mathbf{r}) + \epsilon^2 \Psi_{nlm}^{(2)}(k, \mathbf{r}) + \dots, \quad (72)$$

$$\Lambda_{nlm}(k) = \Lambda_{nlm}^{(0)}(k) + \epsilon \Lambda_{nlm}^{(1)}(k) + \epsilon^2 \Lambda_{nlm}^{(2)}(k) + \dots, \quad (73)$$

where $\Lambda_{nlm}^{(0)}(k) = \lambda_{nl}(k)$. Similarly, we write

$$K_{nlm} = K_{nlm}^{(0)} + \epsilon K_{nlm}^{(1)} + \epsilon^2 K_{nlm}^{(2)} + \dots, \quad (74)$$

with $K_{nlm}^{(0)} = k_{nl}$. Suppose that by using standard techniques we have calculated the first two terms of the expansion (73).

Substituting (74) into (71) and using (73), we obtain

$$\begin{aligned} & (k_{nl} + \epsilon K_{nlm}^{(1)} + \epsilon^2 K_{nlm}^{(2)} + \dots)^2 \\ &= \lambda_{nl}(k_{nl} + \epsilon K_{nlm}^{(1)} + \epsilon^2 K_{nlm}^{(2)} + \dots) \\ &+ \epsilon \Lambda_{nlm}^{(1)}(k_{nl} + \epsilon K_{nlm}^{(1)} + \epsilon^2 K_{nlm}^{(2)} + \dots) \\ &+ \epsilon^2 \Lambda_{nlm}^{(2)}(k_{nl} + \epsilon K_{nlm}^{(1)} + \epsilon^2 K_{nlm}^{(2)} + \dots) + \dots \end{aligned} \quad (75)$$

Expanding the functions on the right side of this equation in Taylor series around $\epsilon = 0$ and equating the terms with the same powers of ϵ on both sides we find, up to and including second-order terms,

$$k_{nl}^2 = \lambda_{nl}(k_{nl}), \quad (76a)$$

$$K_{nlm}^{(1)} = \frac{\Lambda_{nlm}^{(1)}(k_{nl})}{2k_{nl} - \left. \frac{d\lambda_{nl}(k)}{dk} \right|_{k=k_{nl}}}, \quad (76b)$$

$$\begin{aligned} K_{nlm}^{(2)} &= \frac{1}{2k_{nl} - \left. \frac{d\lambda_{nl}(k)}{dk} \right|_{k=k_{nl}}} \\ &\times \left\{ \Lambda_{nlm}^{(2)}(k_{nl}) + K_{nlm}^{(1)} \left. \frac{d\Lambda_{nlm}^{(1)}(k)}{dk} \right|_{k=k_{nl}} \right. \\ &\left. - (K_{nlm}^{(1)})^2 \left[1 - \frac{1}{2} \left. \frac{d^2\lambda_{nl}(k)}{dk^2} \right|_{k=k_{nl}} \right] \right\}. \end{aligned} \quad (76c)$$

The two terms

$$\left. \frac{d\lambda_{nl}(k)}{dk} \right|_{k=k_{nl}} \quad \text{and} \quad \left. \frac{1}{2} \frac{d^2\lambda_{nl}(k)}{dk^2} \right|_{k=k_{nl}} \quad (77)$$

can be calculated substituting the Taylor expansion of $\lambda_{nl}(k)$ around $k = k_{nl}$, into $F_l(n_1\sqrt{\lambda(k)}a, ka) = 0$, and equating to zero the terms with the same power of $(k - k_{nl})$. After a straightforward calculation we find

$$\left. \frac{d\lambda_{nl}(k)}{dk} \right|_{k=k_{nl}} = -\frac{2k_{nl}}{n_1} \rho(k_{nl}), \quad (78)$$

and

$$\begin{aligned} \left. \frac{1}{2} \frac{d^2\lambda_{nl}(k)}{dk^2} \right|_{k=k_{nl}} &= \frac{\rho^2(k_{nl})}{n_1^2} - \frac{k_{nl}a}{n_1} \frac{1}{\left. \frac{\partial F_l(z, k_{nl}a)}{\partial z} \right|_{z=n_1k_{nl}a}} \\ &\times \left[\frac{\partial^2 F_l(z, w)}{\partial w^2} - 2 \frac{\partial^2 F_l(z, w)}{\partial z \partial w} \rho(k_{nl}) \right. \\ &\left. + \frac{\partial^2 F_l(z, w)}{\partial z^2} \rho^2(k_{nl}) \right]_{z=n_1k_{nl}a, w=k_{nl}a}, \end{aligned} \quad (79)$$

where

$$\rho(k_{nl}) \equiv \frac{\left. \frac{\partial F_l(n_1k_{nl}a, w)}{\partial w} \right|_{w=k_{nl}a}}{\left. \frac{\partial F_l(z, k_{nl}a)}{\partial z} \right|_{z=n_1k_{nl}a}}. \quad (80)$$

Incidentally, we note that iterating this procedure it is possible to calculate the function $\lambda_{nl}(k)$ in the neighborhood of any point k_{nl} with the desired degree of accuracy.

Equations (76) are the main result of this section; they formally solve completely our problem. The zeroth-order

Eq. (76a) simply reproduces the resonances of the unperturbed system. The other two equations give first- and second-order corrections in terms of the two functions $\Lambda_{nlm}^{(1)}(k)$ and $\Lambda_{nlm}^{(2)}(k)$ that will be explicitly calculated in the next section. The physical meaning of the denominator in (76b) is explained in [37]; it amounts to a renormalization factor connecting Kapur-Peierls eigenmodes with Gamow (i.e., decaying) modes. The second and third term within the curly brackets in (76c) represent second-order corrections that, in general, should not be neglected with respect to $\Lambda_{nlm}^{(2)}(k_{nl})$.

V. RAYLEIGH-SCHRÖDINGER PERTURBATION THEORY

In this section we use Rayleigh-Schrödinger perturbation theory to find the optical resonances of a deformed dielectric sphere. The only (trivial) difference with respect to familiar quantum perturbation theory is the use of biorthogonal bases [13,15].

Let us consider a specific unperturbed resonant wave number k_{nl} where n and l have now fixed values. The corresponding unperturbed Kapur-Peierls eigenvalue is $\lambda_{nl}(k)$, which we assume to be nondegenerate at the interesting values of k . Here, with “nondegenerate” we mean that there is a single radial wave function $\phi_{nl}(k, r)$ defined by (69) and associated with the eigenvalue $\lambda_{nl}(k)$ via the eigenproblem (68) [37]. However, there are $2l + 1$ different solutions of (68) associated with the same eigenvalue $\lambda_{nl}(k)$, which are obtained by multiplying the unique radial wave function $\phi_{nl}(k, r)$ by the $2l + 1$ angular-dependent spherical harmonics $Y_{lm}(\hat{\mathbf{r}})$:

$$\{\Phi_{nlm}(k, \mathbf{r})\} = \{\phi_{nl}(k, r)Y_{l,-l}(\hat{\mathbf{r}}), \dots, \phi_{nl}(k, r)Y_{ll}(\hat{\mathbf{r}})\}. \quad (81)$$

These solutions span a $(2l + 1)$ -dimensional degenerate subspace, which we call \mathcal{D}_{nl} . According to degenerate perturbation theory, we build the new set of eigenfunctions $\{\Phi_{nlm}^{\mathcal{D}}(k, \mathbf{r})\} \in \mathcal{D}_{nl}$, defined by

$$\{\Phi_{nlm}^{\mathcal{D}}(k, \mathbf{r})\} = \{\phi_{nl}(k, r)\mathcal{Y}_{l,-l}(\hat{\mathbf{r}}), \dots, \phi_{nl}(k, r)\mathcal{Y}_{ll}(\hat{\mathbf{r}})\}, \quad (82)$$

where

$$\mathcal{Y}_{lm}(\hat{\mathbf{r}}) \equiv \sum_{m'=-l}^l C_{lm}^{m'} Y_{lm'}(\hat{\mathbf{r}}). \quad (83)$$

As usual, the coefficients $C_{lm}^{m'}$ can be determined solving the eigenvalue equation

$$\sum_{m''=-l}^l (\tilde{\Phi}_{nlm'}, V^{(1)}(\mathbf{r}) \Phi_{nlm''})_{\mathbf{r}} C_{lm}^{m''} = \Lambda_{nlm}^{(1)}(k) C_{lm}^{m'}, \quad (84)$$

where here and hereafter we use the shorthand notation

$$\begin{aligned} (u, w)_{\mathbf{r}} &\equiv \int_0^a dr \int_0^{2\pi} d\phi \int_0^\pi d\theta \sin\theta u^*(r, \theta, \phi) w(r, \theta, \phi), \\ (u, w)_{\hat{\mathbf{r}}} &\equiv \int_0^{2\pi} d\phi \int_0^\pi d\theta \sin\theta u^*(\theta, \phi) w(\theta, \phi) \end{aligned} \quad (85)$$

(note that the radial differential is dr and not $r^2 dr$). Substituting (69) and (64) into (84) and solving it for $\Lambda_{nlm}^{(1)}(k)$, we obtain the first-order correction to k_{nl} :

$$\Lambda_{nlm}^{(1)}(k) = -a v(k) \phi_{nl}^2(k, a) \ell_{lm}, \quad (86)$$

where $v(k) = k^2(n_1^2 - n_2^2)/n_1^2$ and

$$\ell_{lm} \equiv (\mathcal{Y}_{lm}, h(\hat{\mathbf{r}})\mathcal{Y}_{lm})_{\hat{\mathbf{r}}}, \quad (87)$$

with $m = -l, -l + 1, \dots, l$. This result allows us to find the first-order corrections $K_{nlm}^{(1)}$ by substituting (86), evaluated at $k = k_{nl}$, into (76b).

It should be noted that although ℓ_{lm} is real by definition $\Lambda_{nlm}^{(1)}(k)$ may not be, because $\phi_{nl}^2(k, a)$ is, in general, a complex number. However, using (19) and (35) it is not difficult to show that, for TE polarization,

$$\frac{-a v(k_{nl}) \phi_{nl}^2(k_{nl}, a)}{2k_{nl} - \left. \frac{d\lambda_{nl}(k)}{dk} \right|_{k=k_{nl}}} = -k_{nl}, \quad (88)$$

and (76b) becomes

$$K_{nlm}^{(1)}(k_{nl}) = -k_{nl} \ell_{lm}. \quad (89)$$

Since ℓ_{lm} is a real number, from (89) and (20) it follows that the Q factor of TE waves is not affected by first-order corrections. However, for TM polarization a simple expression such as (89) does not exist because the left side of (88) displays a complicated functional dependence on k_{nl} that will not be reported here. This implies that the Q factor of TM waves may be affected by first-order corrections.

The independence of ℓ_{lm} from the wave number k , the polarization p , the refractive index n_1 , and the radial part of the radial function $\phi_{nl}(k, r)$ is a surprising result of first-order perturbation theory, which was discovered in the 1990s [2,22].

A. Discussion of the first-order corrections

From the definition (87) and (55) it follows that ℓ_{lm} is a real number independent of k and coincides with the m th eigenvalue of the $(2l + 1) \times (2l + 1)$ Hermitian matrix H_l defined by

$$[H_l]_{mm'} = (Y_{lm}, h(\hat{\mathbf{r}})Y_{lm'})_{\hat{\mathbf{r}}}, \quad (m, m' = -l, \dots, l). \quad (90)$$

Moreover, for fixed l and m the coefficients $C_{lm}^{m'}$ in (83) coincide with the components $(C_{lm}^{-l}, C_{lm}^{-l+1}, \dots, C_{lm}^l)$ of the m th eigenvector \mathbf{C}_{lm} associated with ℓ_{lm} , namely, $H_l \mathbf{C}_{lm} = \ell_{lm} \mathbf{C}_{lm}$.

The matrix elements (90) can be calculated from (55) and expressed in terms of the Wigner 3j symbols [45] as

$$\begin{aligned} (Y_{lm}, h(\hat{\mathbf{r}})Y_{lm'})_{\hat{\mathbf{r}}} &= (-1)^m (2l + 1) \sum_{L=2}^{\infty} \sqrt{\frac{2L + 1}{4\pi}} \begin{pmatrix} l & l & L \\ 0 & 0 & 0 \end{pmatrix} \sum_{M=-L}^L h_{LM} \begin{pmatrix} l & l & L \\ -m & m' & M \end{pmatrix} \\ &= (-1)^m (2l + 1) \sum_{l'=1}^l h_{2l', m-m'} \sqrt{\frac{4l' + 1}{4\pi}} \begin{pmatrix} l & l & 2l' \\ 0 & 0 & 0 \end{pmatrix} \begin{pmatrix} l & l & 2l' \\ -m & m' & m - m' \end{pmatrix}, \end{aligned} \quad (91)$$

where the second expression follows from the properties of the $3j$ symbols requiring that only terms with L even, $L \leq 2l$, and $M = m - m'$ contribute to $[H_l]_{mm'}$. This means that at first-order level the resonance k_{nl} is not affected by ‘‘rapid’’ surface fluctuations characterized by $L > 2l$.

The matrix H_l can be huge. For a ^4He droplet of radius $a = 1$ mm, refractive index $n_1 \approx 1.03$, and illuminated by light of wavelength $\lambda = 1$ μm in vacuum, the value of l is around $l \approx 2\pi a n_1 / \lambda \approx 6500$ [1]. Diagonalizing a matrix of dimension

$\sim 10^4 \times 10^4$ with sufficient accuracy may be a serious task depending on the distribution of the matrix elements and on available computational resources. We discuss a way to circumvent these problems in Appendix C.

B. Second-order corrections

Because of the form (63) of the perturbation, the second-order correction $\Lambda_{nlm}^{(2)}(k)$ contains two terms:

$$\begin{aligned} \Lambda_{nlm}^{(2)}(k) &= (\tilde{\Phi}_{nlm}^{\mathcal{D}}, V^{(2)}(\mathbf{r})\Phi_{nlm}^{\mathcal{D}})_{\mathbf{r}} + \sum_{n', l', m' \notin \mathcal{D}_n} \frac{(\tilde{\Phi}_{nlm}^{\mathcal{D}}, V^{(1)}(\mathbf{r})\Phi_{n'l'm'})_{\mathbf{r}} (\tilde{\Phi}_{n'l'm'}, V^{(1)}(\mathbf{r})\Phi_{nlm}^{\mathcal{D}})_{\mathbf{r}}}{\lambda_{nl}(k) - \lambda_{n'l'}(k)} \\ &\equiv A_m(k) + B_m(k). \end{aligned} \quad (92)$$

Using (64) and (82) we can rewrite the first term in the equation above as

$$A_m(k) = -a^2 v(k) \phi_{nl}(k, a) \phi'_{nl}(k, a) T_{lm}, \quad (93)$$

where we have defined

$$T_{lm} \equiv (\mathcal{Y}_{lm}, h^2(\hat{\mathbf{r}})\mathcal{Y}_{lm})_{\hat{\mathbf{r}}}, \quad (94)$$

and $\phi'_{nl}(k, a) = d\phi_{nl}(k, r)/dr|_{r=a}$. Similarly, after a straightforward calculation we obtain, for the second term,

$$B_m(k) = a^2 v^2(k) \phi_{nl}^2(k, a) \sum_{l'} \left[\sum_{n'} \frac{\phi_{n'l'}^2(k, a)}{\lambda_{nl}(k) - \lambda_{n'l'}(k)} T_{lm}^{l'} \right], \quad (95)$$

where

$$T_{lm}^{l'} \equiv \sum_{m'=-l'}^{l'} |(Y_{l'm'}, h(\hat{\mathbf{r}})\mathcal{Y}_{lm})_{\hat{\mathbf{r}}}|^2, \quad (96)$$

and the prime symbols above the sums in l' and n' dictate the exclusion of the term with $(n', l') = (n, l)$. These sums are really formidable and, for high values of l , represent a hard numerical challenge. However, a huge simplification can be made by noticing that after replacing everywhere k with k_{nl} the sum with respect to n' with $l' \neq l$ in (95) can be rewritten as

$$\sum_{n'} \frac{\phi_{n'l'}^2(k_{nl}, a)}{k_{nl}^2 - \lambda_{n'l'}(k_{nl})} = G_{l'}(k_{nl}, a, a), \quad (97)$$

where (76a) has been used and $G_{l'}(k_{nl}, a, a) \equiv G_{l'}(k_{nl})$ is the Green’s function defined in Sec. III C. Comparing this equation with (51) and (52) we obtain a closed expression for the infinite sum (97):

$$G_{l'}(k_{nl}) = \frac{a n_1^2 j_{l'}(n_1 k_{nl} a) h_{l'}^{(1)}(k_{nl} a)}{f_{l'}(k_{nl} a)}, \quad (98)$$

where $f_{l'}(k_{nl} a)$ is the Jost function defined by (17). Therefore, we can eventually rewrite (95) as

$$B_m = a^2 v^2(k) \phi_{nl}^2(k, a) \left[\sum_{n' \neq n} \frac{\phi_{n'l'}^2(k_{nl}, a)}{k_{nl}^2 - \lambda_{n'l'}(k_{nl})} T_{lm}^{l'} + \sum_{l' \neq l} G_{l'}(k_{nl}) T_{lm}^{l'} \right]. \quad (99)$$

Eventually, the awkward double sum in (95) was split into two simpler single sums, one with respect to $n' \neq n$ and the other with respect to $l' \neq l$.

VI. APPLICATIONS

Our results are in agreement with previous works where first-order perturbation theory for leaking electromagnetic modes in open systems was developed [2,22]. This is shown in the first two following examples. In the third and last example

we apply our perturbation theory to the case of a dielectric sphere (glass) with surface roughness.

A. Equatorial bulge

Consider a TE excitation of the droplet; this sets $p = 1$. Suppose that $h(\hat{\mathbf{r}})$ describes an ellipsoid of revolution with polar and equatorial radii a_p and $a_E > a_p$, respectively, with $a_p a_E^2 = a^3$. The ellipticity (or eccentricity) of this ellipsoid is

denoted e and defined by

$$e = \sqrt{1 - \frac{a_P^2}{a_E^2}}. \quad (100)$$

The surface profile function of the ellipsoid of revolution is

$$a + ah(\hat{\mathbf{r}}) = \frac{a_P a_E}{\sqrt{a_E^2 \cos^2 \theta + a_P^2 \sin^2 \theta}}, \quad (101)$$

which, when $e \ll 1$, can be approximated by

$$h(\hat{\mathbf{r}}) \cong -\frac{e^2}{12}[1 + 3 \cos(2\theta)] = -\frac{2}{3}\sqrt{\frac{\pi}{5}} e^2 Y_{20}(\hat{\mathbf{r}}). \quad (102)$$

Then, from this equation and (91) it follows that

$$(Y_{lm}, h(\hat{\mathbf{r}})Y_{lm'})_{\hat{\mathbf{r}}} = \delta_{mm'} \frac{e^2}{3} \frac{l(l+1) - 3m^2}{4l(l+1) - 3}. \quad (103)$$

Substituting (103) into (89) we obtain, for $l \gg 1$,

$$\frac{K_{nlm}^{(1)}(k_{nl})}{k_{nl}} = -\frac{e^2}{12} \left[1 - \frac{3m^2}{l(l+1)} \right], \quad (104)$$

which is in perfect agreement with [22] (note: because of a different definition, the parameter e used in [22] is equal to our $e^2/2$).

B. Shrinking sphere

As a second example, consider as a perturbation the change of the radius of the sphere from a to $b < a$, such that $a - b \equiv \delta a \ll a$. Let z_{nl} be a root of the equation (19) $f_l(z) = 0$ with $p = 1$ (TE polarization) and denote with $k_{nl}(a) \equiv z_{nl}/a$ and $k_{nl}(b) \equiv z_{nl}/b$ the two corresponding resonances of the bigger and smaller cavity. Then, trivially,

$$\begin{aligned} k_{nl}(b) &= \frac{k_{nl}(a)}{1 - \frac{\delta a}{a}} \\ &\cong k_{nl}(a) \left(1 + \frac{\delta a}{a} + \frac{\delta a^2}{a^2} + \dots \right) \\ &\equiv k_{nl}(a) + K_{nlm}^{(1)} + K_{nlm}^{(2)} + \dots \end{aligned} \quad (105)$$

The surface profile function (54) of the sphere of radius b is evidently $g(\hat{\mathbf{r}}) = b$. This implies that $h(\hat{\mathbf{r}}) = -\delta a/a$. The matrix H_l has elements $[H_l]_{mm'} = -(\delta a/a)\delta_{mm'}$ and, therefore, $\ell_{lm} = -\delta a/a$. A straightforward calculation shows that

$$T_{lm} = (\delta a/a)^2 \quad \text{and} \quad T_{lm}' = (\delta a/a)^2 \delta_{ll'}. \quad (106)$$

Then, (87) yields

$$K_{nlm}^{(1)} = k_{nl}(a) \frac{\delta a}{a}, \quad (107)$$

in perfect agreement with (105). From (76) we obtain

$$k_{nl}(b) \cong k_{nl}(a) \left(1 + \frac{\delta a}{a} + N_{nl} \frac{\delta a^2}{a^2} \right), \quad (108)$$

where N_{nl} is a finite complex-valued numerical coefficient that can be calculated explicitly once n and l have been fixed. Equation (108) is in agreement with (105) up to $O(\delta a^2/a^2)$ corrections.

C. Surface roughness

As we remarked in the introduction, typical systems to which our theory can be applied are drops of different kinds of liquids ranging from water at room temperature (think of, e.g., raindrops) to liquid helium at few hundreds of millikelvin. As a matter of fact, raindrops or any other kind of droplets are only approximately spherical. For example, the shape of the millimeter-size drops of liquid helium magnetically levitated in vacuum that we considered in [11] deviates from the spherical one because of two different physical processes. First, rotation of the droplet leads to an equatorial bulge; this changes the droplet's free surface from spherical to oblate. The effects of this kind of deformation upon the optical resonances of a dielectric sphere have been already extensively investigated in [22]. Second, thermally excited capillary waves (ripples) result in an effective stochastic surface roughness of the droplet. Therefore, to further illustrate our theory in this part we study the effects of surface roughness upon the resonances of a dielectric sphere immersed in vacuum.

To begin with, let us consider the deviation of a dielectric particle from the spherical shape caused by a surface roughness which is described by (54) and (55) with random coefficients h_{LM} . These are generated as detailed in Appendix D, with

$$g_L = g \frac{1}{L(L+1) - 2}, \quad (109)$$

where g determines the “strength” of the roughness. In our numerical calculations we take $g = 10^{-6}$ (according to (D4) for a He droplet of radius $a = 500$ nm, the value $g = 10^{-6}$ corresponds to a temperature of about 7 Kelvin). However, as with $\Lambda_{nm}^{(1)} \propto g$ and $\Lambda_{nm}^{(2)} \propto g^2$, we have the freedom to adjust the value of g at our will after numerical evaluations (we shall use this feature later). For the sake of definiteness, we consider a single realization of surface randomness obtained by generating one set of $(L_{\text{Max}} - 1)(L_{\text{Max}} + 3)$ random complex numbers $\{h_{LM}\}$. From (D1) it follows that the simplest deformation which breaks all rotational symmetries is achieved taking $L_{\text{max}} = 3$. This is just enough to split the degenerate wave number k_{nl} into $(2l + 1)$ distinct values: $k_{nl} \rightarrow K_{nlm} = \{K_{nl,-l}, K_{nl,-l+1}, \dots, K_{nl,l}\}$. However, as we shall show later, some wave numbers remain close in pairs, that is, $K_{nlm} \cong K_{nl,m+1}$ for some values of m . Numerical explorations show that once the “optical” l is fixed we must take the “acoustic” $L_{\text{max}} \gtrsim 2l$ to further split the remaining quasidegenerate pairs of wave numbers.

The flow of calculations goes as follows: first, using (90) and (91) we evaluate the $(2l + 1) \times (2l + 1)$ Hermitian matrix H_l , the elements of which are determined by the previously generated random set $\{h_{LM}\}$, and we diagonalize it:

$$H_l \mathbf{u}_i = \lambda_i \mathbf{u}_i, \quad (i = 1, \dots, 2l + 1). \quad (110)$$

To perform this operation we write H_l according to (90) as

$$H_l = \begin{bmatrix} [H_l]_{-l,-l} & [H_l]_{-l,-l+1} & \cdots & [H_l]_{-l,l} \\ [H_l]_{-l+1,-l} & [H_l]_{-l+1,-l+1} & \cdots & [H_l]_{-l+1,l} \\ \vdots & \vdots & \ddots & \vdots \\ [H_l]_{l,-l} & [H_l]_{l,-l+1} & \cdots & [H_l]_{l,l} \end{bmatrix} \equiv \begin{bmatrix} [H_l]_{11} & [H_l]_{12} & \cdots & [H_l]_{1,2l+1} \\ [H_l]_{21} & [H_l]_{22} & \cdots & [H_l]_{2,2l+1} \\ \vdots & \vdots & \ddots & \vdots \\ [H_l]_{2l+1,1} & [H_l]_{2l+1,2} & \cdots & [H_l]_{2l+1,2l+1} \end{bmatrix}. \quad (111)$$

The above identification $[H_l]_{mm'} \equiv [H_l]_{ij}$ automatically fixes the following invertible relations between the two sets of indices $\{m, m'\}$ and $\{i, j\}$:

$$\begin{cases} i = m + l + 1, \\ j = m' + l + 1, \end{cases} \quad \begin{cases} m = i - l - 1, \\ m' = j - l - 1. \end{cases} \quad (112)$$

Then, from this result and (83) it follows that the new basis functions \mathcal{Y}_{lm} for the degenerate subspace can be written as

$$\mathcal{Y}_{lm}(\hat{\mathbf{r}}) \equiv \sum_{m'=-l}^l [\mathbf{u}_{m+l+1}]^{m'+l+1} Y_{lm'}(\hat{\mathbf{r}}), \quad (113)$$

where $m = -l, \dots, l$ and $[\mathbf{u}_i]^j$ denotes the j th component of the i th eigenvector of H_l . Of course the (arbitrary) sorting of these functions $\{\mathcal{Y}_{l,-l}, \mathcal{Y}_{l,-l+1}, \dots, \mathcal{Y}_{ll}\} = \{\mathcal{Y}_{l,1}, \mathcal{Y}_{l,2}, \dots, \mathcal{Y}_{l,2l+1}\}$ is uniquely determined by the way we sort the eigenvalues of H_l . In our calculations we fix $\lambda_1 < \lambda_2 < \dots < \lambda_{2l+1}$. The eigenvalue λ_i determines the first-order

correction $\{K_{nlm}^{(1)}\}$ according to (76b) and (86), where

$$\Lambda_{nlm}^{(1)}(k_{nl}) = -a v(k_{nl}) \phi_{nl}^2(k_{nl}, a) \lambda_{m+l+1}, \quad (114)$$

with $m = -l, -l+1, \dots, l$. So, the net result of first-order perturbation is to split the $(2l+1)$ -fold degenerate wave number k_{nl} into $2l+1$ distinct values:

$$k_{nl} \rightarrow \{k_{nl} + K_{nl,-l}^{(1)}, \dots, k_{nl} + K_{nl,l}^{(1)}\}. \quad (115)$$

The successive step is the calculation of the $2l+1$ coefficients T_{lm} given by (94). Substituting (113) into (94) we obtain

$$T_{lm} = \sum_{m'=-l}^l \sum_{m''=-l}^l [\mathbf{u}_{m+l+1}^*]^{m'+l+1} [\mathbf{u}_{m+l+1}]^{m''+l+1} \times (Y_{lm'}, h^2(\hat{\mathbf{r}}) Y_{lm''})_{\hat{\mathbf{r}}}. \quad (116)$$

The calculation of the last factor involves the integral over the unit sphere of the product of four spherical harmonics and can be quite time consuming. So, we found it convenient to evaluate such an expression analytically using the Wigner $3j$ symbols [45]:

$$(Y_{lm'}, h^2(\hat{\mathbf{r}}) Y_{lm''})_{\hat{\mathbf{r}}} = (-1)^{m'} \frac{2l+1}{4\pi} \sum_{L=2}^{L_{\text{Max}}} \sqrt{2L+1} \sum_{L'=2}^{L_{\text{Max}}} \sqrt{2L'+1} \sum_{M=-L}^L \sum_{M'=-L'}^{L'} \left\{ h_{LM} h_{L'M'} \sum_{l''=0}^{2l} \times (2l'+1) \begin{pmatrix} l & l & l' \\ 0 & 0 & 0 \end{pmatrix} \begin{pmatrix} l & l & l' \\ -m' & m'' & m' - m'' \end{pmatrix} \begin{pmatrix} l' & L & L' \\ 0 & 0 & 0 \end{pmatrix} \begin{pmatrix} l' & L & L' \\ m'' - m' & M & M' \end{pmatrix} \right\}. \quad (117)$$

The last coefficients to calculate are the $T_{lm}^{l'}$ s given by (96):

$$T_{lm}^{l'} = \sum_{m'=-l'}^{l'} |(Y_{l'm'}, h(\hat{\mathbf{r}}) \mathcal{Y}_{lm})_{\hat{\mathbf{r}}}|^2, \quad (118)$$

where

$$(Y_{l'm'}, h(\hat{\mathbf{r}}) \mathcal{Y}_{lm})_{\hat{\mathbf{r}}} = \sum_{m''=-l}^l [\mathbf{u}_{m+l+1}]^{m''+l+1} (Y_{l'm'}, h(\hat{\mathbf{r}}) Y_{lm''})_{\hat{\mathbf{r}}}. \quad (119)$$

The calculation of the term $(Y_{l'm'}, h(\hat{\mathbf{r}}) Y_{lm''})_{\hat{\mathbf{r}}}$ may look non-trivial because, in principle, l' can take any non-negative integer value besides $l' = l$. However, substituting (55) into

the expression above we find

$$(Y_{l'm'}, h(\hat{\mathbf{r}}) Y_{lm''})_{\hat{\mathbf{r}}} = (-1)^{m'} \sqrt{\frac{(2l+1)(2l'+1)}{4\pi}} \sum_{L=2}^{L_{\text{Max}}} h_{L,m'-m''} \sqrt{2L+1} \times \begin{pmatrix} l' & L & l \\ 0 & 0 & 0 \end{pmatrix} \begin{pmatrix} l' & L & l \\ -m' & m' - m'' & m'' \end{pmatrix}. \quad (120)$$

From this equation and the symmetry properties of the Wigner $3j$ symbols, it follows that $|L-l| \leq l' \leq L+l$. Therefore, in (95) the sum $\sum_{l'}$ can be replaced by

$$\sum_{l'=0}^{\infty} \rightarrow \sum_{l'=L-l}^{L+l}, \quad (121)$$

where the prime symbol in both sums denotes $l' \neq l$.

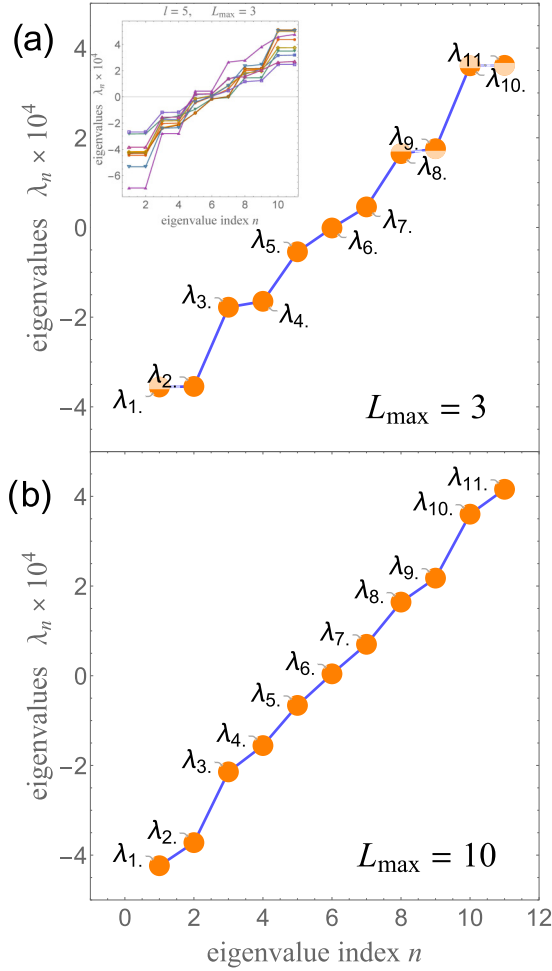


FIG. 4. (a) Diagram showing the 11 eigenvalues of the $(2l + 1) \times (2l + 1)$ matrix H_l , with $l = 5$, averaged over 10^2 realizations of the random coefficients h_{LM} , for $L_{\max} = 3$. These eigenvalues are calculated according to (110). Such diagonalization in the $(2l + 1)$ -fold degenerate subspace associated with the unperturbed wave number k_{nl} leads, via (114), to the first-order splitting of k_{nl} . Inset: Ten different realizations of the eigenvalues of H_l illustrating their statistical variance. The random coefficients h_{LM} are generated as described in Appendix D with $g = 10^{-6}$. (b) Same as in panel (a) but for $L_{\max} = 10$. When L_{\max} substantially exceeds l the degeneracy is completely removed.

Having calculated the coefficients T_{lm} we can straightforwardly obtain $A_m(k_{nl})$ from (93) evaluated at $k = k_{nl}$. Next, the knowledge of T_{lm}' permits us to evaluate $B_m(k_{nl})$ from (99). For practical purposes it is convenient to rewrite

$$B_m(k_{nl}) = B_0(k_{nl})[B_{m1}(k_{nl}) + B_{m2}(k_{nl})], \quad (122)$$

where $B_0 \equiv a^2 v^2(k_{nl}) \phi_{nl}^2(k_{nl}, a)$, and

$$B_{m1}(k_{nl}) \equiv T_{lm}^l \sum_{n' \neq n} \frac{\phi_{n'l}^2(k_{nl}, a)}{k_{n'l}^2 - \lambda_{n'l}(k_{nl})}, \quad (123)$$

$$B_{m2}(k_{nl}) \equiv \sum_{l'=|L-l|}^{L+1} G_{l'}(k_{nl}) T_{lm}', \quad (124)$$

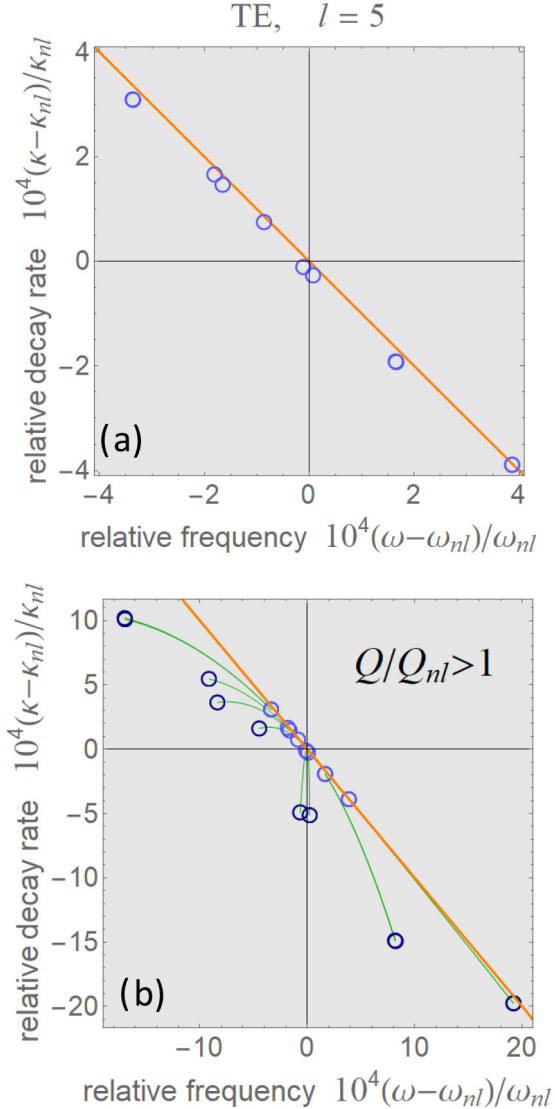


FIG. 5. (a) Light blue circles: Perturbed wave numbers K_{nlm} for TE polarization, $l = 5$, and surface roughness strength $g = 10^{-6}$. In this figure $\omega = c \operatorname{Re} K_{nlm}$, $\omega_{nl} = c \operatorname{Re} k_{nl}$, $\kappa = -2c \operatorname{Im} K_{nlm}$, $\kappa_{nl} = -2c \operatorname{Im} k_{nl}$, and the wave number k_{nl} of the unperturbed sphere is located at the origin of the coordinate system. The diagonal orange line divides the upper region, characterized by $Q > Q_{nl}$, from the lower one where $Q < Q_{nl}$, where $Q = \omega/\kappa$ and $Q_{nl} = \omega_{nl}/\kappa_{nl}$. (b) Light blue circles, as in panel (a); dark blue circles, as in panel (a) but for surface roughness strength $g = 25 \times 10^{-6}$; continuous green lines, the “motion” of the perturbed wave numbers when g increases by a factor 25.

with $m = -l, -l + 1, \dots, l$. The calculation of $B_{m2}(k_{nl})$ is straightforward, but the sum in (123) requires numerical evaluation of $\lambda_{n'l}(k_{nl})$. These quantities are obtained by solving numerically with respect to z the transcendental equation

$$n_1 z j_{l+1}(n_1) h_l^{(1)}(x) - x j_l(n_1 z) h_{l+1}^{(1)}(x) = 0, \quad (125)$$

for TE polarization, and

$$n_1 z j_{l+1}(n_1) h_l^{(1)}(x) + j_l(n_1 z) \times [(l+1)(n_1^2 - 1) h_l^{(1)}(x) - n_1^2 x h_{l+1}^{(1)}(x)] = 0, \quad (126)$$

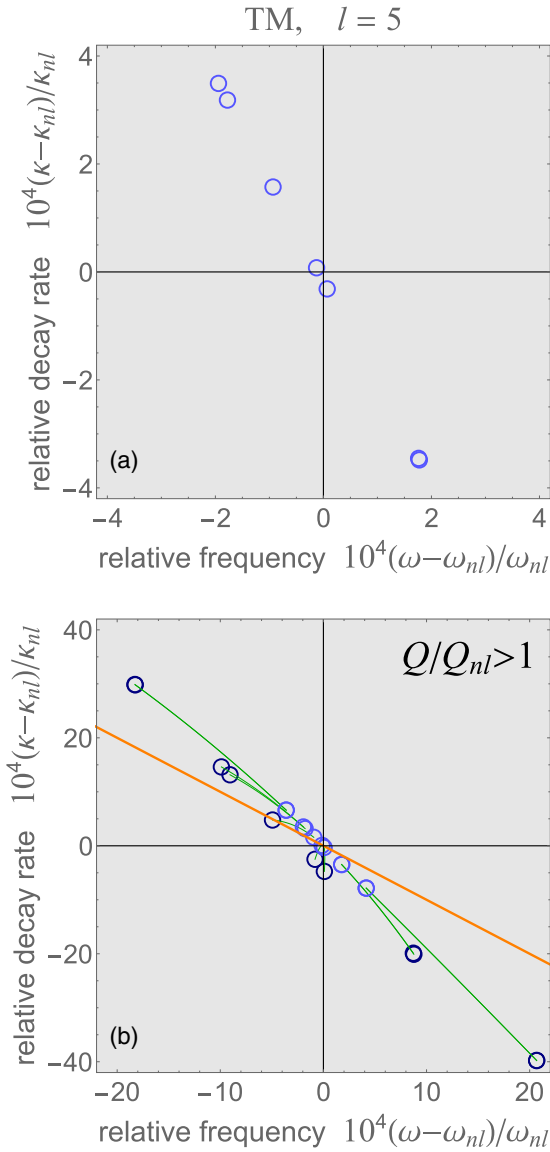


FIG. 6. As in Fig. 5 but for TM polarization.

for TM polarization. In these two equations $x = ak_{nl}$. Let $z_{n'}$ be a solution of one of these equations. Then $\lambda_{n'l}(k_{nl})$ is simply determined from $z_{n'} = a\sqrt{\lambda_{n'l}(k_{nl})}$. In principle the sum in (123) is extended to all the infinite integer values of n' , which is the label for the solutions of either (125) and (126). However, in practice, we must truncate the sum to some finite value of n' . For our calculations we have chosen $\max\{n'\} = 10^4$ to guarantee a good accuracy.

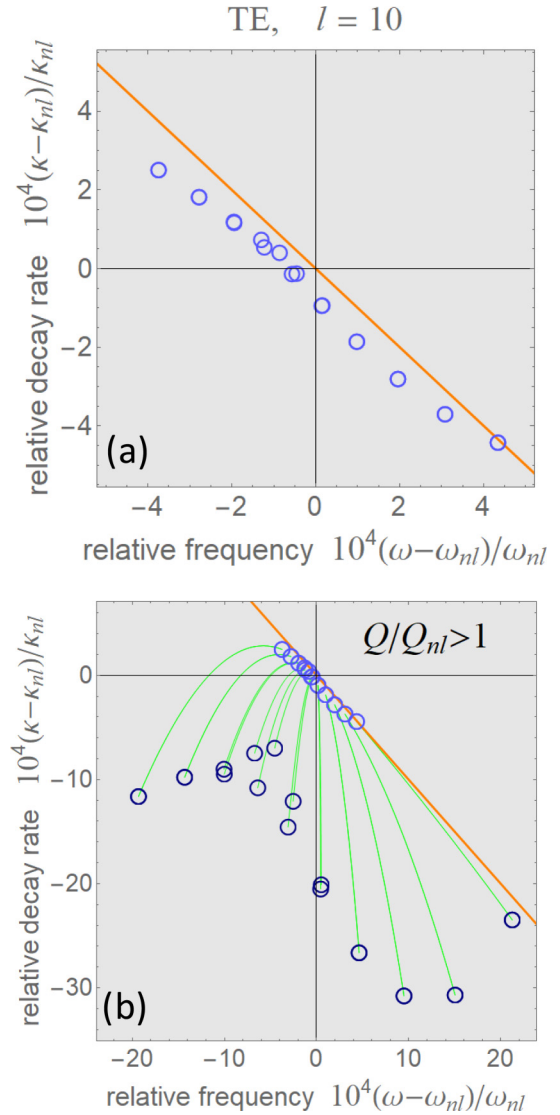
Finally, to calculate $B_{m1}(k_{nl})$ we need also to evaluate $\phi_{n'l}(k_{nl}, a)$. From (35) and (36) it straightforwardly follows that

$$\phi_{n'l}(k_{nl}, a) = \frac{1}{\sqrt{Z_{n'l}}} a j_l(n_1 z_{n'}), \quad (127)$$

where

$$Z_{n'l} = \frac{a^3}{2} [j_l^2(n_1 z_{n'}) - j_{l-1}(n_1 z_{n'}) j_{l+1}(n_1 z_{n'})], \quad (128)$$

and, as previously defined, $z_{n'} = a\sqrt{\lambda_{n'l}(k_{nl})}$.

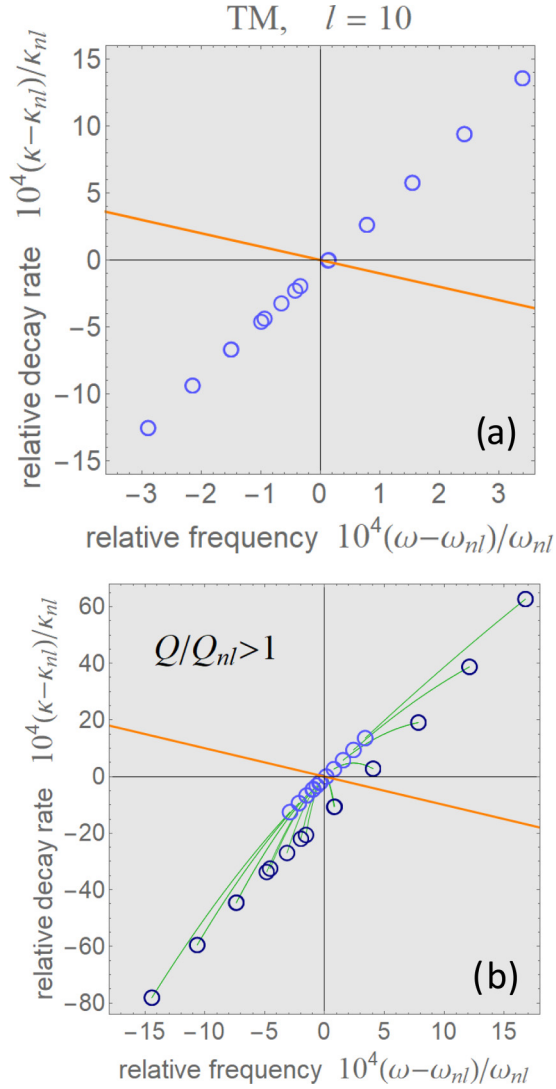

 FIG. 7. As in Fig. 5 but for $l = 10$.

Numerical results and plots

For illustration we study here the effects of surface roughness upon two optical modes with $l = 5$, $l = 10$, and both TE and TM polarizations, of a glass sphere of refractive index $n_1 = 1.5$, in vacuum.

A key step in the perturbation theory illustrated above is the calculation of the eigenvalues of H_l . In Fig. 4 we show the 11 eigenvalues of H_5 averaged over 10^2 realizations of the random coefficients h_{LM} , with $L_{\max} = 3$ [Fig. 4(a)] and $L_{\max} = 10$ [Fig. 4(b)]. Figure 4(a) shows that for $L_{\max} \lesssim l$ the pairs of eigenvalues (λ_1, λ_2) , (λ_3, λ_4) , (λ_8, λ_9) , and $(\lambda_{10}, \lambda_{11})$ are almost degenerate, that is, very close in value but still unambiguously distinct within the numerical precision. Therefore, we treat these eigenvalues as nondegenerate. However, as shown in Fig. 4(b), when $L_{\max} > l$ all the eigenvalues become well distinct.

The perturbed wave numbers K_{nlm} calculated from (74) and (76a)–(76c) are shown in Figs. 5 and 6 for $l = 5$ and TE and TM polarization, respectively. Similarly, Figs. 7 and 8 depict the values of K_{nlm} for $l = 10$ and TE and TM polarization,


 FIG. 8. As in Fig. 6 but for $l = 10$.

respectively. Here and hereafter $\omega = c \operatorname{Re} K_{nlm}$, $\omega_{nl} = c \operatorname{Re} k_{nl}$ and $\kappa = -2c \operatorname{Im} K_{nlm}$, $\kappa_{nl} = -2c \operatorname{Im} k_{nl}$. In these figures the diagonal orange lines divide the complex plane into two regions: the upper part consists of points for which $Q > Q_{nl}$, where $Q = \omega/\kappa$ and $Q_{nl} = \omega_{nl}/\kappa_{nl}$, and the lower part consists of points such that $Q < Q_{nl}$. For TE polarization all the perturbed wave numbers give $Q < Q_{nl}$. However, for TM polarization the values below the diagonal correspond to modes with $Q < Q_{nl}$, but the values located above the diagonal give $Q > Q_{nl}$. The origin of such different wave-number distributions for TE and TM waves is due to the different values taken by the left side of (88). In the TE case, (88) is simply equal to $-k_{nl}$, which implies that $Q = Q_{nl}$ at first-order perturbation theory, as shown by (89). However, in the TM case the left side of (88) is a complex number different from $-k_{nl}$:

$$\begin{aligned}
 & \frac{-a v(k_{nl}) \phi_{nl}^2(k_{nl}, a)}{2k_{nl} - \left. \frac{d\lambda_{nl}(k)}{dk} \right|_{k=k_{nl}}} \\
 & \simeq \begin{cases} 5.68 \exp(i\pi 0.94), & l = 5, \\ 5.89 \exp(-i\pi 0.97), & l = 10. \end{cases} \quad (129)
 \end{aligned}$$

In panels (b) of Figs. 5–8 we show the evolution of the resonant wave numbers when the strength of the surface roughness increases from g to $25g$. The light blue circles at the beginning of the continuous green curves mark the wave numbers evaluated at g [as in panels (a) of the figures]. The dark blue circles at the end of the same curves mark the wave numbers evaluated at $25g$. These figures show that, as expected, when g increases, the separation between adjacent wave numbers grows.

VII. SUMMARY

In this paper we have used the Kapur-Peierls formalism, originally developed in the context of nuclear scattering theory, to find the optical resonances of almost spherical dielectric objects, such as liquid drops. This permitted us to develop a second-order perturbation theory for the electromagnetic Debye potentials describing the light fields. We have thus found analytical formulas for the complex characteristic values of the resonances, the real and imaginary parts of which are proportional to, respectively, the central frequency and the bandwidth of the optical resonance. When limited to first-order perturbation theory, our results are in perfect agreement with older results [22]. The present paper provides the basis for applications of our technique to various optical and optomechanical systems.

ACKNOWLEDGMENTS

A.A. and F.M. were supported by the European Union's Horizon 2020 Research and Innovation program under Grant No. 732894, Future and Emerging Technologies (FET)-Proactive Hybrid Optomechanical Technologies (HOT). A.A. is grateful to Carlos Viviescas for useful discussions. J.H. acknowledges Charles Brown for his contribution and support, W. M. Keck Foundation Grant No. DT121914, AFOSR Grant No. FA9550-15-1-0270, Defense Advanced Research Project Agency Grant No. W911NF-14-1-0354, and NSF Grant No. 1205861. This project was made possible through the support of a grant from the John Templeton Foundation.

APPENDIX A: SPHERICAL BESSEL AND HANKEL FUNCTIONS

Spherical Bessel and Hankel functions are frequently encountered in scattering theory. Many of their properties can be found in Appendix A of [30] and in Appendix A.9 of [46]. Some properties utilized in this paper are as follows.

(1) Recurrence:

$$j_{l-1}(z) = \frac{2l+1}{z} j_l(z) - j_{l+1}(z). \quad (A1)$$

(2) Differentiation:

$$z j_{l+1}(z) = (l+1) j_l(z) - \frac{d}{dz} [z j_l(z)]. \quad (A2)$$

(3) Parity:

$$j_l(-z) = (-1)^l j_l(z), \quad (A3a)$$

$$y_l(-z) = (-1)^{l+1} y_l(z), \quad (A3b)$$

$$h_l^{(1)}(-z) = (-1)^l h_l^{(2)}(z). \quad (A3c)$$

(4) Analytic continuation:

$$[j_l(z)]^* = j_l(z^*), \quad (\text{A4a})$$

$$[y_l(z)]^* = y_l(z^*), \quad (\text{A4b})$$

$$j_l(-z^*) = (-1)^l [j_l(z)]^*, \quad (\text{A4c})$$

$$y_l(-z^*) = (-1)^{l+1} [y_l(z)]^*, \quad (\text{A4d})$$

$$h_l^{(\alpha)}(-z^*) = (-1)^l [h_l^{(\alpha)}(z)]^*, \quad (\alpha = 1, 2), \quad (\text{A4e})$$

$$[h_l^{(1)}(z)]^* = h_l^{(2)}(z^*). \quad (\text{A4f})$$

(5) Integrals:

$$\begin{aligned} & \int_0^a j_l(xr) j_l(yr) r^2 dr \\ &= \frac{a^2}{x^2 - y^2} [y j_l(xa) j_{l-1}(ya) - x j_{l-1}(xa) j_l(ya)], \quad (\text{A5a}) \end{aligned}$$

$$\begin{aligned} & \int_0^a j_l^2(xr) r^2 dr \\ &= \frac{a^3}{2} [j_l^2(xa) - j_{l-1}(xa) j_{l+1}(xa)]. \quad (\text{A5b}) \end{aligned}$$

Relations 1 and 2 also hold for $y_l(z)$, $h_l^{(1)}(z)$, and $h_l^{(2)}(z)$.

APPENDIX B: TE AND TM RESONANCES OF A DIELECTRIC SPHERE

The complex-valued resonances of the sphere are generally associated with the poles of the scattering amplitudes (16). These poles are found by solving with respect to the complex variable $z = a(k' + ik'') \equiv x + iy$ the transcendental equation

$$\begin{aligned} f_l(z) &= p j_l(n_1 z) [z h_l^{(1)}(z)]' - h_l^{(1)}(z) [(n_1 z) j_l(n_1 z)]' \\ &= 0, \quad (\text{B1}) \end{aligned}$$

where $p = 1$ for TE polarization and $p = n_1^2/n_2^2$ for TM polarization. Equation (19) admits solutions only for certain *characteristic values* of the complex variable z . These characteristic values form a denumerable set $\{z_{0l}, z_{\pm 1l}, z_{\pm 2l}, \dots, z_{\pm nl}, \dots\}$, where $\text{Re } z_{nl} = -\text{Re } z_{-nl} > 0$ and $\text{Im } z_{nl} < 0$, for all n . We label the poles with $\text{Re } k < 0$ by the negative index $-n$, so that $k_{-nl} = -k_{nl}^*$. For l odd (even) and TE (TM) polarization there exists a pole denoted k_{0l} such that $\text{Re } k_{0l} = 0$ and $\text{Im } k_{0l} < 0$. Figure 9 shows two typical distributions, symmetric with respect to the vertical axis, for TE and TM polarization, of the roots of $f_l(z)$ in the complex k plane for a glass sphere of radius a , refractive index $n_1 = 1.5$, and azimuthal number $l = 10$. Filled and open black circles mark, respectively, characteristic values z^R and z^{NR} associated with resonant and nonresonant modes of the field. The latter are very leaky modes that are sometimes called *external whispering gallery modes* [47]. Grandy [30] suggested that to distinguish between resonant and nonresonant characteristic values one should evaluate (i) the phase shift δ_l , (ii) the scattering strength $\sin^2 \delta_l$, (iii) the interior wave amplitude $|A_l|$, and (iv) the *specific time delay*

$$\tau_l \equiv \frac{1}{a} \frac{d\delta_l}{dk} = \frac{1}{2i} \frac{d}{d(ka)} \log S_l. \quad (\text{B2})$$

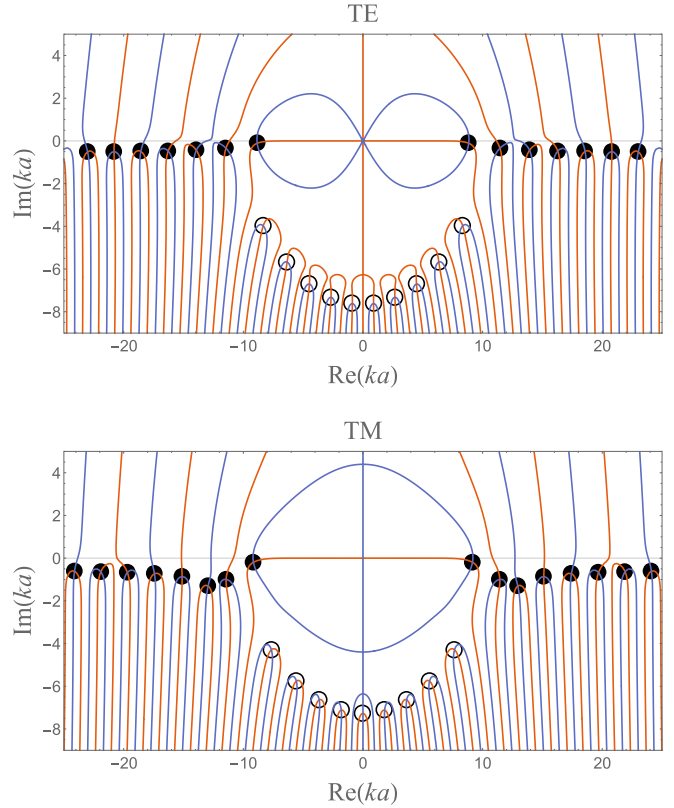


FIG. 9. Contour plots in the complex k plane of the zeros of $f_l(z)$ for TE (top) and TM (bottom) polarization. Points on the red curves are solutions of the equation $\text{Re } f_l(z) = 0$ and points on the blue curves are solutions of $\text{Im } f_l(z) = 0$. The characteristic values z_{nl} are those points where red and blue lines cross each other. Filled circles mark resonant values z^R ; open circles indicate nonresonant values z^{NR} . In this figure, $n_1 = 1.5$ and $l = 10$. Values of k with larger real part correspond to higher radial quantum number, where one expects the modes to become more lossy.

However, it is possible to show that these conditions are almost equivalent [48] and that, for example, it is sufficient to verify the presence of a sharp peak in τ_l per each value of $ka = \text{Re } z^R$, as shown in Fig. 10. In practice, we wish z_{1l}^R to be the pole with $\text{Re } z_{1l}^R \sim 1/n_1$ and the smallest imaginary part (the subsequent resonant values will be ordered according to $\text{Re } z_{1l}^R < \text{Re } z_{2l}^R < \dots$, etc.). Therefore, the resonant z_{nl}^R can be found by comparing the solutions of (19) with the characteristic values of TE and TM modes of the *same* dielectric sphere but embedded in a medium of infinite conductivity (closed sphere), these values having null imaginary parts. They are the real-valued solutions $\{x_{1l}, x_{2l}, \dots, x_{nl}, \dots\}$, with $x_{1l} < x_{2l} < \dots$, of [29]:

$$\begin{cases} j_l(n_1 x) = 0, & \text{TE polarization,} \\ [(n_1 x) j_l(n_1 x)]' = 0, & \text{TM polarization.} \end{cases} \quad (\text{B3})$$

Thus, we *define* z_{1l}^R as the solution of $f_l(z) = 0$ closest to the smaller root x_{1l} of (B3), namely,

$$z_{1l}^R = \{z \in \mathbb{C} \mid f_l(z) = 0, \text{Re } z > 0, |z - x_{1l}| = \min\}. \quad (\text{B4})$$

Then, given a solution z of $f_l(z) = 0$, $z = z^R$ if either $\text{Re } z > \text{Re } z_{1l}^R$ or $\text{Re } z < -\text{Re } z_{1l}^R$, because z and $-z^*$ are solutions

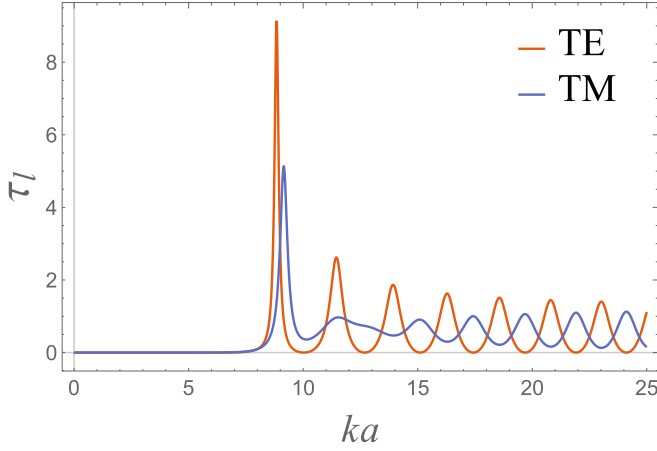


FIG. 10. Plot of the specific time delay (B2) for a glass sphere of radius a , refractive index $n_1 = 1.5$, and azimuthal number $l = 10$. Red curve, TE polarization; blue curve, TM polarization. The peaks of these curves are located at $ka = \text{Re } z^R$, where z^R denotes a solution of (19) associated with a resonant mode of the field.

of the same equation. This empirical rule is illustrated in Fig. 11, which shows the location in the complex k plane of a few solutions of (B1) (filled and open red circles) and (B3) (blue squares on the real axis) for a glass sphere of radius a , refractive index $n_1 = 1.5$, and azimuthal number $l = 10$.

APPENDIX C: PERTURBATIVE DIAGONALIZATION OF H_l

In many cases of practical interest (as, e.g., in He droplets [11]), the “deformation” function $h(\hat{\mathbf{r}})$ is made of two contributions. The first one is deterministic and describes an equatorial bulge due to, for example, the rotation of the droplet and is denoted with $h_{\text{rot}}(\hat{\mathbf{r}})$. The second contribution may be stochastic and generated by surface waves (rippions) on the droplet. Let us denote with $h_{\text{rip}}(\hat{\mathbf{r}})$ this second term. As typically $|h_{\text{rip}}(\hat{\mathbf{r}})| \ll |h_{\text{rot}}(\hat{\mathbf{r}})|$, we can diagonalize H_l using perturbation theory after defining

$$H_l = H_l^{(0)} + H_l^{(1)}, \quad (\text{C1})$$

where

$$\begin{aligned} [H_l^{(0)}]_{mm'} &= (Y_{lm}, h_{\text{rot}}(\hat{\mathbf{r}})Y_{lm'})_{\hat{\mathbf{r}}} = \delta_{mm'} \ell_{l|m|}^{(0)}, \\ [H_l^{(1)}]_{mm'} &= (Y_{lm}, h_{\text{rip}}(\hat{\mathbf{r}})Y_{lm'})_{\hat{\mathbf{r}}}, \end{aligned} \quad (\text{C2})$$

with $\ell_{l|m|}^{(0)}$ defined by (103). If $m \neq 0$ each eigenvalue of $H_l^{(0)}$ is doubly degenerate and (87) can be approximately rewritten as

$$\ell_{lm} \approx \ell_{l|m|}^{(0)} + \ell_{l,\pm|m|}^{(1)}, \quad (\text{C3})$$

where $\ell_{l,+|m|}^{(1)}$ and $\ell_{l,-|m|}^{(1)}$ denote the eigenvalues of the 2×2 matrix $H_{lm}^{(1)}$ defined by

$$H_{lm}^{(1)} \equiv \begin{bmatrix} (Y_{lm}, h_{\text{rip}}(\hat{\mathbf{r}})Y_{lm})_{\hat{\mathbf{r}}} & (Y_{lm}, h_{\text{rip}}(\hat{\mathbf{r}})Y_{l,-m})_{\hat{\mathbf{r}}} \\ (Y_{l,-m}, h_{\text{rip}}(\hat{\mathbf{r}})Y_{lm})_{\hat{\mathbf{r}}} & (Y_{l,-m}, h_{\text{rip}}(\hat{\mathbf{r}})Y_{l,-m})_{\hat{\mathbf{r}}} \end{bmatrix}, \quad (\text{C4})$$

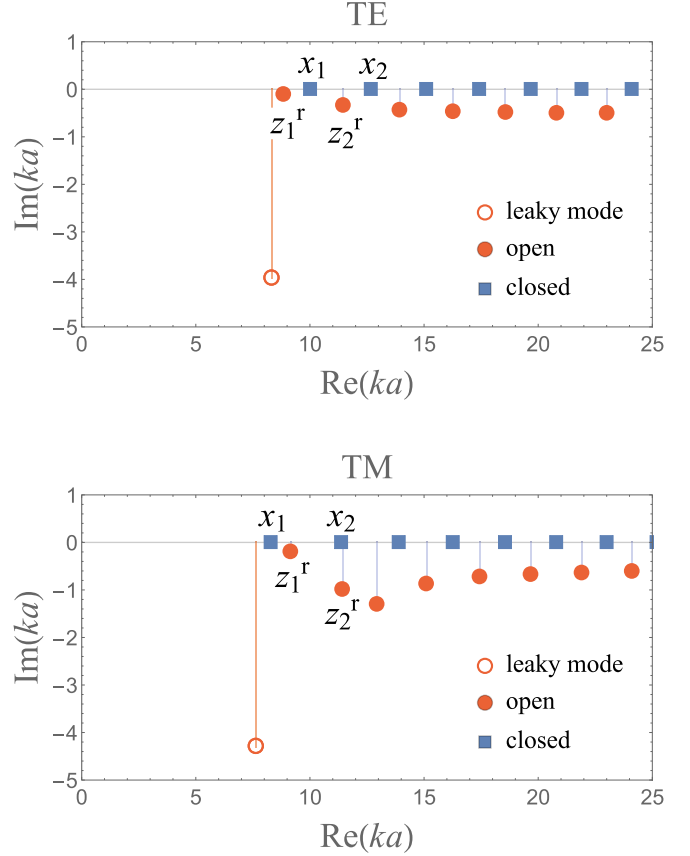


FIG. 11. Characteristic values for (B1) (filled and open red circles) and (B3) (blue squares on the real axis) as given in Fig. 9 for $\text{Re}(ka) > 0$. Top, TE polarization; bottom, TM polarization. The first two resonances of an open (z_1^R and z_2^R) and a closed (x_1 and x_2) sphere are marked. In this figure we have chosen the same parameters as in Fig. 9, that is, $n_1 = 1.5$ and $l = 10$. For the sake of clarity we have omitted the index l in the plots.

with $m = 1, 2, \dots, l$. Explicitly,

$$\ell_{l,\pm|m|}^{(1)} = \frac{1}{2}(H_{11} + H_{22} \pm \Delta), \quad (\text{C5})$$

where here and hereafter we use the shorthand notation $[H_{lm}^{(1)}]_{ij} \equiv H_{ij}$, ($i, j = 1, 2$), and

$$\Delta = \sqrt{(H_{11} - H_{22})^2 + 4|H_{12}|^2}. \quad (\text{C6})$$

If $m = 0$ we can apply nondegenerate perturbation theory to obtain

$$\ell_{l0} \approx \ell_{l0}^{(0)} + (Y_{l0}, h_{\text{rip}}(\hat{\mathbf{r}})Y_{l0})_{\hat{\mathbf{r}}}. \quad (\text{C7})$$

Similarly, the functions $\mathcal{Y}_{lm}(\hat{\mathbf{r}})$ spanning the degenerate subspace \mathcal{D}_{nl} can be approximated by

$$\mathcal{Y}_{lm}(\hat{\mathbf{r}}) \approx Y_{lm}(\hat{\mathbf{r}}) + (1 - \delta_{m0})\mathcal{Y}_{l,\pm|m|}^{(0)}(\hat{\mathbf{r}}), \quad (\text{C8})$$

where

$$\mathcal{Y}_{l,\pm|m|}^{(0)}(\hat{\mathbf{r}}) = C_{1\pm}Y_{l|m|}(\hat{\mathbf{r}}) + C_{2\pm}Y_{l,-|m|}(\hat{\mathbf{r}}), \quad (\text{C9})$$

with the superscript “(0)” marking the zeroth-order character of these corrections, and

$$\begin{aligned} C_{1\pm} &= \sqrt{\frac{H_{12}}{2|H_{12}|} \left(1 \pm \frac{H_{11} - H_{22}}{\Delta}\right)}, \\ C_{2\pm} &= \pm \sqrt{\frac{H_{21}}{2|H_{21}|} \left(1 \mp \frac{H_{11} - H_{22}}{\Delta}\right)}. \end{aligned} \quad (\text{C10})$$

APPENDIX D: DESCRIPTION OF THE EFFECTIVE STOCHASTIC SURFACE ROUGHNESS

We describe the surface roughness of the sphere by the random function

$$h(\hat{\mathbf{r}}) = \sum_{L=2}^{L_{\text{Max}}} \sum_{M=-L}^L h_{LM} Y_{LM}(\hat{\mathbf{r}}), \quad (\text{D1})$$

where the reality constraint $h(\hat{\mathbf{r}}) = h^*(\hat{\mathbf{r}})$ entails $h_{LM}^* = (-1)^M h_{L,-M}$. The value of L_{Max} is determined by the physical process generating the roughness. For example, the roughness could be caused by a stationary, stochastic process, characterized by

$$\overline{h(\hat{\mathbf{r}})} = 0, \quad (\text{D2a})$$

$$\overline{h(\hat{\mathbf{r}})h(\hat{\mathbf{r}}')} = \sum_{L=2}^{L_{\text{Max}}} g_L P_L(\cos \gamma), \quad (\text{D2b})$$

where the overbar denotes the statistical average over the ensemble of realizations of the surface profile, $P_L(\cos \gamma)$ is the L -degree Legendre polynomial, and $\cos \gamma = \hat{\mathbf{r}} \cdot \hat{\mathbf{r}}'$ [49]. From (D2b) and $P_L(1) = 1$, it follows that the coefficients g_L obey the sum rule:

$$\overline{h^2(\hat{\mathbf{r}})} = \sum_{L=2}^{\infty} g_L \equiv \Delta^2, \quad (\text{D3})$$

where Δ denotes the standard deviation and quantifies the magnitude of the surface roughness. The coefficients g_L actually determine the properties of the rough surface and must be such that the sum (D3) converges to a finite value. For example, if the dielectric sphere represents a ^4He droplet at

temperature T with random deformation induced by thermally excited ripples we have, according to [2],

$$g_L = \frac{k_B T}{\gamma_S a^2} \frac{1}{L(L+1) - 2}, \quad (\text{D4})$$

where γ_S the surface tension of the liquid and k_B is the Boltzmann constant. In this case a straightforward calculation shows that

$$\sum_{L=2}^{\infty} g_L = \frac{k_B T}{\gamma_S a^2} \frac{11}{18}. \quad (\text{D5})$$

Substituting (D1) into (D2) we determine the statistical properties of the real random variables $U_{LM} = \text{Re}(h_{LM})$ and $V_{LM} = \text{Im}(h_{LM})$. After a straightforward calculation we obtain $\overline{U_{LM}} = 0 = \overline{V_{LM}}$, and

$$\overline{U_{LM}U_{L'M'}} = \frac{2\pi}{2L+1} g_L (1 + \delta_{M0}) \delta_{LL'} \delta_{MM'}, \quad (\text{D6a})$$

$$\overline{V_{LM}V_{L'M'}} = \frac{2\pi}{2L+1} g_L \delta_{LL'} \delta_{MM'}, \quad (\text{D6b})$$

$$\overline{U_{LM}V_{L'M'}} = 0. \quad (\text{D6c})$$

For numerical simulations, we found it convenient to model U_{LM} and V_{LM} as Gaussian random variables distributed according to the probability density function

$$f(x; \mu, \sigma) = \frac{1}{\sqrt{2\pi}\sigma} \exp\left[-\frac{(x - \mu)^2}{2\sigma^2}\right], \quad (\text{D7})$$

with $\mu = 0$ and

$$\sigma^2 = \begin{cases} \overline{U_{LM}^2}, & \text{if } x = U_{LM}, \\ \overline{V_{LM}^2}, & \text{if } x = V_{LM}, \end{cases} \quad (\text{D8})$$

where (D6) have been used. Once these numbers have been generated we write

$$h_{LM} = \begin{cases} U_{LM} + iV_{LM}, & M > 0, \\ U_{L0}, & M = 0, \\ (-1)^M (U_{L,-M} - iV_{L,-M}), & M < 0. \end{cases} \quad (\text{D9})$$

-
- [1] A. N. Oraevsky, *Quantum Electron.* **32**, 377 (2002).
 [2] H. M. Lai, P. T. Leung, and K. Young, *Phys. Rev. A* **41**, 5199 (1990).
 [3] A. Chiasera, Y. Dumeige, P. Féron, M. Ferrari, Y. Jestin, G. Nunzi Conti, S. Pelli, S. Soria, and G. Righini, *Laser Photonics Rev.* **4**, 457 (2010).
 [4] Raymond L. Lee, Jr. and Alistair B. Fraser, *The Rainbow Bridge: Rainbows in Art, Myth, and Science* (Pennsylvania State University, University Park, Pennsylvania, 2001).
 [5] M. R. Foreman, J. D. Swaim, and F. Vollmer, *Adv. Opt. Photon.* **7**, 168 (2015).
 [6] G. Lin, A. Coillet, and Y. K. Chembo, *Adv. Opt. Photon.* **9**, 828 (2017).
 [7] M. Aspelmeyer, T. J. Kippenberg, and F. Marquardt, *Rev. Mod. Phys.* **86**, 1391 (2014).
 [8] M. Aspelmeyer, T. J. Kippenberg, and F. Marquardt (Eds.), *Cavity Optomechanics*, Quantum Science and Technology (Springer-Verlag, Berlin, 2014).
 [9] S.-X. Qian, J. B. Snow, H.-M. Tzeng, and R. K. Chang, *Science* **231**, 486 (1986).
 [10] R. Dahan, L. L. Martin, and T. Carmon, *Optica* **3**, 175 (2016).
 [11] L. Childress, M. P. Schmidt, A. D. Kashkanova, C. D. Brown, G. I. Harris, A. Aiello, F. Marquardt, and J. G. E. Harris, *Phys. Rev. A* **96**, 063842 (2017).
 [12] C. W. Gardiner, *Handbook of Stochastic Methods*, Springer Series in Synergetics, 2nd ed. (Springer-Verlag, Berlin, 2002).
 [13] M. M. Sternheim and J. F. Walker, *Phys. Rev. C* **6**, 114 (1972).
 [14] I. Rotter, *J. Phys. A: Math. Theor.* **42**, 153001 (2009).
 [15] D. C. Brody, *J. Phys. A: Math. Theor.* **47**, 035305 (2014).

- [16] V. I. Kukulin, V. M. Krasnopol'sky, and J. Horáček, *Theory of Resonances*, Reidel Texts in the Mathematical Sciences (Springer, New York, 1989).
- [17] G. Gamow, *Z. Phys.* **51**, 204 (1928).
- [18] A. J. F. Siegert, *Phys. Rev.* **56**, 750 (1939).
- [19] P. Lind, *Phys. Rev. C* **47**, 1903 (1993).
- [20] E. A. Muljarov, W. Langbein, and R. Zimmermann, *Europhys. Lett.* **92**, 50010 (2010).
- [21] M. B. Doost, W. Langbein, and E. A. Muljarov, *Phys. Rev. A* **90**, 013834 (2014).
- [22] H. M. Lai, P. T. Leung, K. Young, P. W. Barber, and S. C. Hill, *Phys. Rev. A* **41**, 5187 (1990).
- [23] A. Bohm, M. Gadella, and G. B. Mainland, *Am. J. Phys.* **57**, 1103 (1989).
- [24] R. de la Madrid, *J. Math. Phys.* **53**, 102113 (2012).
- [25] P. L. Kapur and R. Peierls, *Proc. R. Soc. A* **166**, 277 (1938).
- [26] R. Peierls, *Math. Proc. Cambridge Philos. Soc.* **44**, 242 (1948).
- [27] C. Viviescas and G. Hackenbroich, *Phys. Rev. A* **67**, 013805 (2003).
- [28] C. Viviescas and G. Hackenbroich, *J. Opt. B* **6**, 211 (2004).
- [29] J. A. Stratton, *Electromagnetic Theory*, IEEE Press Series on Electromagnetic Wave Theory (Wiley, New York, 2007).
- [30] W. T. Grandy, *Scattering of Waves from Large Spheres* (Cambridge University, Cambridge, England, 2000).
- [31] A. Zangwill, *Modern Electrodynamics* (Cambridge University, Cambridge, England, 2013).
- [32] J. D. Jackson, *Classical Electrodynamics*, 3rd ed. (Wiley, New York, 2001).
- [33] B. R. Johnson, *J. Opt. Soc. Am. A* **10**, 343 (1993).
- [34] R. G. Newton, *Scattering Theory of Waves and Particles*, 2nd ed. (Dover, New York, 2002).
- [35] J. Giambiagi and T. Kibble, *Ann. Phys.* **7**, 39 (1959).
- [36] D. V. Savin, V. V. Sokolov, and H.-J. Sommers, *Phys. Rev. E* **67**, 026215 (2003).
- [37] R. M. More and E. Gerjuoy, *Phys. Rev. A* **7**, 1288 (1973).
- [38] G. E. Brown, *Rev. Mod. Phys.* **31**, 893 (1959).
- [39] R. Johnson, *Kapur-Peierls, Wigner-Eisenbud, and All That*, University of Surrey, Surrey, England, http://www.nucleartheory.net/Talent_6_Course/Other_materials/Johnson/ronsnotes.pdf.
- [40] L. Fonda, G. C. Ghirardi, T. Weber, and A. Rimini, *J. Math. Phys.* **7**, 1643 (1966).
- [41] C. L. Dolph, *Bull. Amer. Math. Soc.* **67**, 1 (1961).
- [42] M. Abramowitz and I. A. Stegun, *Handbook of Mathematical Functions*, Riccati-Bessel Functions Sec. 10.3, 10th ed. (Dover, New York, 1972), p. 445.
- [43] E. W. Weisstein, Heaviside step function, *MathWorld—A Wolfram Web Resource*, <http://mathworld.wolfram.com/HeavisideStepFunction>.
- [44] L. O. Krainov, P. A. Batishchev, and O. I. Tolstikhin, *Phys. Rev. A* **93**, 042706 (2016).
- [45] E. W. Weisstein, Wigner 3j-Symbol, *MathWorld—A Wolfram Web Resource*, <http://mathworld.wolfram.com/Wigner3j-Symbol.html>.
- [46] Alberto Galindo and Pedro Pascual, *Quantum Mechanics I*, Texts and Monographs in Physics (Springer-Verlag, Berlin, 1990).
- [47] R. Dubertrand, E. Bogomolny, N. Djellali, M. Lebental, and C. Schmit, *Phys. Rev. A* **77**, 013804 (2008).
- [48] H. C. Ohanian and C. G. Ginsburg, *Am. J. Phys.* **42**, 310 (1974).
- [49] G. Farias, E. Vasconcelos, S. Cesar, and A. Maradudin, *Physica A (Amsterdam)* **207**, 315 (1994).